4 Higher-layer issues: ad hoc and sensor networks

Maria-Gabriella Di Benedetto, Luca De Nardis, and Salvatore Falco

4.1. Introduction

Ultra-wide-band (UWB) radio has the potential of allowing simultaneous communication of a large number of users at high bit rates [1–3]. In addition, the high temporal resolution inherent to UWB provides robustness against multipath fading and is particularly attractive for indoor local area network (LAN) applications. UWB is also capable of recovering distance information with great precision. As we will show later in this chapter, distance and position data can lead to better organization of wireless networks, for instance, through better resource management and routing [4]. UWB signals spread, however, over very large bandwidths and overlap with narrowband services. As a consequence, regulatory bodies impose severe limitations on UWB power density in order to avoid interference provoked by UWB onto coexisting narrowband systems [5]. It is therefore necessary to take into account power considerations when designing UWB systems. Throughout this chapter we will show how the distance information made available by the UWB technology can be exploited to achieve low power levels and increase network lifetime in the long term, while providing an adequate network performance (in terms of data throughput) in the short term.

In the last few years, the increasing interest in applications based on the deployment of ad hoc networks triggered significant research efforts regarding the introduction of the energy-awareness concept in the design of medium access control (MAC) and routing protocols. Ad hoc networks are in fact considered as a viable solution for scenarios in which fixed infrastructure, and consequently unlimited power sources, are not available. In such scenarios, an efficient management of the limited power supply available in each terminal is a key element for achieving acceptable network lifetimes. This is particularly true for sensor networks, for which long battery duration is one of the basic requirements, given the typical size of such networks (up to thousands of terminals), as will be analyzed in Section 4.2.

Location information is another valuable way of achieving energy-awareness in ad hoc networks. In Section 4.3 we first review location-aware routing protocols

with focus on power efficiency. We then address the problem of information exchange through the network by means of specifically designed protocols.

Next, we introduce in Section 4.4 a MAC protocol which foresees a dedicated procedure for the acquisition of distance information and which is tailored on UWB features.

The last section of the chapter, Section 4.5, analyzes the effect of mobility on the behavior of the proposed MAC and routing strategies.

4.2. Power-efficient UWB networks

4.2.1. Introduction

This section briefly illustrates the current research trends regarding power-efficient MAC, and power-efficient routing strategies.

4.2.2. Power-efficient MAC

As far as power-aware MAC design is concerned, most of the research activity took the moves from existing solutions for medium access in wireless networks, and in particular carrier sensing multiple access (CSMA), and out-of-band signaling.

CSMA is based on a channel sensing period performed by each terminal before starting transmission. The performance obtained by CSMA is however heavily affected by two phenomena, the well-known "hidden terminal" and "exposed terminal" problems. In order to solve the hidden and exposed terminal problems, solutions that substitute CSMA have been proposed. The multiple access with collision avoidance (MACA) protocol [6], for example, replaces the carrier sensing procedure with a three-way handshake between transmitter and receiver. Following this approach, further modifications of the MACA protocol have been developed, such as MACAW [7] and MACA-by invitation (MACA-BI) [8].

Practical implementations of MAC protocols combine handshake and carrier sensing, as proposed in the floor acquisition multiple access (FAMA) protocol [9]. These protocols are commonly referred to as CSMA with collision avoidance (CSMA-CA). An example of CSMA-CA is the distributed foundation wireless MAC (DFWMAC), which has been adopted for the MAC layer of the 802.11 IEEE standard [10].

An alternative solution to CSMA-CA is offered by the out-of-band signaling protocol [11]. This solution splits the available bandwidth into two channels: a data channel used for data packet exchange, and a narrowband signaling channel on which sinusoidal signals (referred to as busy tones) are asserted by terminals that are transmitting and/or receiving, in order to avoid interference produced by hidden terminals. In order to reduce the number of exposed terminals, the use of two different *busy tones* for transmitting and receiving terminals was proposed in [12].

CSMA-CA is by far the most common approach adopted in narrowband wireless LANs. This family of protocols suffers, however, from several drawbacks in

terms of power consumption: packet collisions, which cause a waste of power due to re-transmission, terminals blocked in idle state by active transmissions, and overhearing, that is, power consumption in the reception of packets by non-intended destinations. Several protocols aiming at solving these drawbacks were proposed. Among all, it is worth mentioning the power-aware multiple access protocol with signaling for ad hoc networks (PAMAS) [13]. This protocol combines the CSMA approach with the out-of-band principle, in order to minimize the time a terminal spends in the idle state without neither transmitting nor receiving. The protocol foresees, in fact, a control channel on which the handshake between transmitter and receiver takes place, and a data channel on which data packets are exchanged. The control channel allows terminals to determine when they may safely switch to sleep mode, saving thus power, without affecting data throughput or end-to-end delay. The main idea behind PAMAS is that if a node detects the channel as busy, it goes in sleep mode rather than waste power in idle mode without being able to exchange data packets. The protocol defines dedicated handshakes, which allow terminals to determine for how long they can keep the radio interface switched off. Simulations show that this approach leads to a power save of up to 70% compared to the standard MACA protocol. It should be noted, however, that part of the dramatic advantage shown by PAMAS over MACA is intrinsically due to the assumption of adopting a CSMA-CA approach at the MAC level. PAMAS exploits, in fact, the presence of "pause" periods in the terminal lifetime, due to busy channel or lost contention, to save energy without affecting delay and throughput. If a different solution, for example, Aloha without carrier sensing, is adopted, the PAMAS-like approach is no longer a suitable option.

4.2.3. Power-efficient routing

Power-efficient routing is another topic which is of great interest in relation to distributed ad hoc and sensor networks. Most of the power-aware protocols proposed in the literature are based either on the definition of power-effective routing metrics or on the exploitation of additional information, such as location of terminals in the network. In both cases, the final aim is to find source-destination paths that minimize power consumption.

Regarding the definition of power-aware routing metrics, [14] provides a thorough analysis of the effect of power-aware metrics on network lifetime and fairness in energy consumption between different terminals in the network. The metrics taken into account in the analysis include transmission power, cumulative transmitted and received power, residual power in each node, and their combinations. Interestingly, simulation results presented in [14] show that a straightforward minimization of transmitted power does not necessarily lead to a longer lifetime for each terminal in the network. The adoption of a power-aware routing metric may in fact give rise to paths composed of a high number of hops, involving thus a higher number of terminals in each communication. This strategy provides however fair power consumption between different terminals, increasing thus the

network operation time before the first terminal runs out of power with the consequence of potentially causing a network partition.

For the specific case of UWB, a method for setting up connections by optimizing a power-dependent cost function is described in [15], and further refined in [16, 17]. In [15], a communication cost is attached to each path, and the cost of a path is the sum of the costs related to the links it comprises. The cost function is expressed as the sum of two components as follows:

$$C(x, y) = \delta \cdot C_0 \cdot d^{\alpha} + C_1 \cdot R \cdot d^{\alpha}. \tag{4.1}$$

The first component takes into account the synchronization cost for setting-up a new link. If two nodes already share an active link, $\delta = 0$ and there is no synchronization cost. If two nodes do not share an active link, $\delta = 1$ and a synchronization cost is added. The second component takes into account the cost for transmitting data, and depends upon the requested data rate R. Both terms are related to power consumption, and therefore depend upon the distance d between two nodes. Note that the evaluation of such a distance relies on the precise ranging capabilities offered by the UWB technique. The parameter α is related to channel propagation characteristics and has commonly a value between 2 and 4. Constants C_0 and C_1 are used to weight the synchronization and transmission components.

In [16] the proposed strategy is compared against traditional routing in a scenario characterized by fixed terminals and full network connectivity. Results show that the power-saving strategy, as expected, leads to multihop communication paths between terminals within reach of each other (physical visibility) and by this way increases network performance by reducing average emitted power and thus interference levels [16]. In [17] an improved version of the cost function was proposed, in order to introduce additional parameters in the route selection metrics. The general form of this cost function is given by

$$C(x, y) = C(\text{power}) + C(\text{sync}) + C(\text{interference}) + C(\text{quality}) + C(\text{delay}), \tag{4.2}$$

where the first two terms, related to power and synchronization, respectively, resemble the two terms defined in (4.1).

The UWB ranging capability is the basis for the definition of the above power aware cost function; ranging information, however, can be even more efficiently exploited to build a network map through a distributed protocol, providing thus the input for a location-based routing algorithm. This topic will be addressed in Section 4.3, which deals with both distributed positioning and location-based routing protocols.

4.3. Location-aware UWB networks

4.3.1. Introduction

As anticipated in Section 4.2, location information is valuable for achieving power-efficiency in ad hoc networks. In this section we investigate how location information can be exploited in UWB networks, thanks to the accurate ranging capability offered by this technique. First, we review location-aware routing protocols available in literature, with focus on power-efficient protocols. Next, we address the topic of how location information can be gathered and exchanged in a UWB network, by providing an example of a GPS-free positioning protocol suitable for a UWB network, and finally we analyze the effect of UWB-based positioning on the location-aware routing protocols originally designed for GPS-enabled terminals.

4.3.2. Location-aware routing protocols

As a general concept, all location-aware routing protocols pursue an improvement of network performance by taking into account location information in the route selection process. Depending on how this information is used, different aspects of the routing performance can be optimized. Section 4.3.2.2, for example, shows how location information can be used for increasing route stability. The main focus being here on power efficiency, however, the remaining part of this section addresses routing protocols that exploit location information for reducing routing overhead, and thus power consumption.

4.3.2.1. Greedy perimeter stateless routing

The greedy perimeter stateless routing (GPSR) [18] protocol uses location information to reduce protocol overhead and obtain a good scalability when both terminal mobility and network size increase. GPSR adopts positional information as the key metric in packet forwarding, and uses the following simple "greedy" forwarding strategy.

(1) Each packet is marked by the source terminal with the latest information about the location of the destination.
(2) Each intermediate node forwards the packet to the neighboring visible node, that is, closest to the location of the destination stored in the packet itself.

Note that greedy forwarding does not guarantee that a path between source and destination is always detected, even if it exists. An example of greedy forwarding failure is presented in Figure 4.1. Node x, after receiving a packet from source S intended for destination D, cannot find a neighbor which satisfies the greedy forwarding rule, since both neighbors y and z are further than x from the destination D.

When greedy forwarding fails, the GPSR protocol switches from greedy forwarding to perimeter forwarding, in which a terminal is allowed to forward the

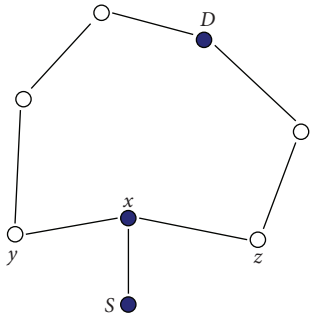

FIGURE 4.1. Example of greedy forwarding failure. Arcs in the figure represent physical visibility between nodes. The greedy forwarding rule fails at node x since both neighbors y and z are further than x from the destination D.

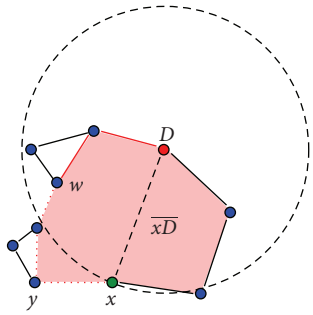

FIGURE 4.2. Combination of perimeter forwarding and greedy forwarding. Arcs in the figure represent physical visibility between nodes. The selected path is represented by a thick line (dotted links: perimeter forwarding, filled links: greedy forwarding).

packet to a neighbor which is further than itself from destination, in order to solve the stall caused by greedy forwarding. The perimeter forwarding strategy uses the so-called right-hand rule to forward packets around the area in which the greedy approach fails, and can be described as follows (see Figure 4.2).

Suppose that x is the first terminal in which greedy forwarding fails.

(1) Terminal x records its position in the apposite L_f field in the packet.
(2) Terminal x uses the information on its location and the location of destination D recorded in the packet to determine the $\overline{xD}$ line.
(3) Terminal x, based on the position of its neighbors, determines which is the first edge in counterclockwise direction from the $\overline{xD}$ line (edge $\overline{xy}$ in Figure 4.2).
(4) Terminal x forwards the packet to terminal y.
(5) Terminal y checks if it is closer to destination D than the position recorded in the L_f field. If this is the case, y switches back to greedy forwarding, otherwise repeats the procedure from step 2.

In the example in Figure 4.2, x enters the perimeter forwarding, and w switches back to the greedy forwarding. The grey area defines the perimeter over which the algorithm switches from greedy forwarding to perimeter forwarding.

4.3.2.2. Location-aware long-lived route selection in wireless ad hoc network

The location-aware long-lived routing (LLR) protocol [19] belongs to the family of source-initiated, on-demand routing protocols. The protocol exploits location information aiming at the minimization of route failures and, as a consequence, of route reconstruction procedures. As in traditional source routing protocols, a source terminal S in need of a route to a destination broadcasts route discovery packets to its neighbors, and the latter will forward packets until the destination is reached.

In LLR, the source S includes two additional information fields in each generated packet: its own position (X_S, Y_S) and radio transmission range R_s. Each terminal A in physical connectivity with S that receives the packet uses such information and its own position (X_A, Y_A) and transmission range R_A to evaluate two figures.

(1) Forward movement limit (FML), that measures the maximum relative movement between A and S which can be tolerated before the distance between A and S is larger than the transmission range of A, defined as

$$\text{FML} = R_A - \text{distance}(A,S) = R_A - \sqrt{(X_S - X_A)^2 + (Y_S - Y_A)^2}. \tag{4.3}$$

(2) Backward movement limit (BML), that measures the maximum relative movement between A and S which can be tolerated before the distance between A and S is larger than the transmission range of S, defined as

$$\text{BML} = R_S - \text{distance}\,(A,S) = R_S - \sqrt{(X_S - X_A)^2 + (Y_S - Y_A)^2}. \tag{4.4}$$

FML and BML are then used to evaluate the normalized movement limit (NML), which provides a single figure averaging FML and BML (note that FML $\neq$ BML when $R_S \neq R_A$):

$$\text{NML} = \frac{\text{FML} \cdot \text{BML}}{\text{FML} + \text{BML}}. \tag{4.5}$$

Terminal A updates the packet by including the NML and substituting (X_A, Y_A) and R_A to (X_S, Y_S) and R_S, respectively, and forwards it to its neighbors.

The NML is an indicator of link stability: the higher the NML value, the lower the probability of link failure due to terminal mobility. When the destination D

receives several route discovery packets originated from the source S, it selects the route characterized by the highest NML, in order to minimize the probability of a route failure. In [19] two alternative ways are foreseen to evaluate the end-to-end reliability of each route, depending on the way a route discovery packet is updated.

Additive NML. Each terminal adds the NML value relative to the last hop to the value carried by the packet, and the best path is characterized by the maximum overall NML.

Min-max NML. Each terminal compares the NML just evaluated with the value recorded in the packet: if the current value is lower than the old one, the packet is updated by overwriting the NML field, otherwise the field is left unchanged. In this case the best route is determined by the worst link in each route (which determines the NML value in the route discovery packet).

4.3.2.3. Distance routing effect algorithm for mobility (DREAM)

The DREAM algorithm [20] proposes the idea of using location information to reduce the amount of routing overhead. The protocol combines both proactive and reactive approaches, by relying on both periodic updates by each terminal for the dissemination of location information and a flooding-like procedure for sending a packet to the targeted destination.

When a source terminal S starts the procedure at $t = t_1$ it is supposed to have the following information:

(i) its own position (X_S, Y_S),
(ii) the positions of its one-hop neighbors,
(iii) the position of the destination D, (X_D, Y_D), at a given time $t_0 < t_1$,
(iv) the maximum speed v of the destination, or at least a probability density function of the speed, $p(v)$.

The source, based on this information, defines a geographical region in which the routing packets should be forwarded, and determines the subset of neighbors that are positioned inside this region, as shown in Figure 4.3. The forwarding region is determined by the angle α.

Depending on the information on destination speed, two cases are possible.

(1) v is known: in this case the distance x traveled by the destination in the period $t_1 - t_0$ is given by $x = v * (t_1 - t_0)$, and, given a distance r between S and D, one has

$$\alpha = \arcsin \frac{x}{r}. \tag{4.6}$$

(2) $p(v)$ is known: in this case in order to determine a forwarding region including D with probability p, the corresponding value of α can be derived from [20]:

$$\int_{r \cdot \sin \alpha/(t_1 - t_0)}^{+\infty} p(v)dv \geq p. \tag{4.7}$$

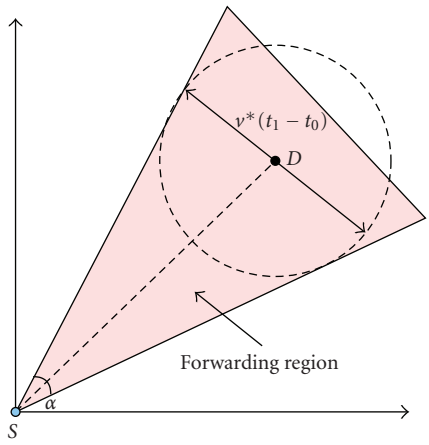

FIGURE 4.3. Definition of the forwarding region in the DREAM protocol.

Once α has been determined, the terminal sends the packet indicating the neighbors lying within the forwarding region. Each intermediate terminal, when receiving a packet, evaluates if the packet should be forwarded by defining its own forwarding region, and by checking if any neighbor lies within it. If no neighbor lies within the forwarding region, the packet is not forwarded, reducing thus the overhead by avoiding packet retransmissions in wrong directions.

As stated before, the procedure requires positional information regarding not only the source, but also its neighbors and destination. This information is exchanged through a distributed dissemination algorithm, which constitutes the proactive routing protocol part.

Each terminal A periodically broadcasts update packets containing its own position; two types of update packets are defined in DREAM:

(i) *short-lived packets*, for updating the location tables in A's neighbors,

(ii) *long-lived packets*, for updating the location tables in terminals that are not in direct connectivity with A.

Note that the lifetime of each packet is defined in terms of physical distance reached from the terminal originating the packet: each terminal B receiving an update packet generated by terminal A checks both A's position (recorded in the packet) and its own position: if the distance between A and B is higher than the packet lifetime, the packet is discarded, otherwise, it is forwarded. Short-lived and long-lived packets are emitted by each terminal with different frequencies, taking into account the so-called distance effect, which is represented in Figure 4.4 and can be described as follows.

Given a terminal A moving at speed v, and two terminals B and C that at $t = t_0$ are positioned at distances D_{AB} and $D_{AC} \gg D_{AB}$ from A, respectively, terminal B will experience a faster variation of the forwarding region to destination A than terminal C, due to A's movement in the time interval $t_1 - t_0$ (i.e., the angle α_B will increase faster than the angle α_C to keep A in the forwarding region). As a

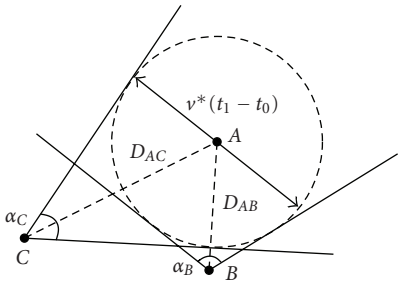

FIGURE 4.4. Example of distance effect. Given two nodes B and C at distances D_{AB} and D_{AC}, with $D_{AC} > D_{AB}$, the angles α_B and α_C as derived either from (4.6) or (4.7) are such that $\alpha_B > \alpha_C$, and B needs thus more frequent updates than C on the position of A, in order to keep A within the forwarding region.

consequence, B will need much more frequent updates than C regarding A's position: such updates will be provided by means of short-lived packets that will reach B without increasing the routing overhead all over the network. C will receive updates at lower frequency by means of long-lived packets.

Each terminal is thus expected to adapt the emission frequencies of both long-lived and short-lived packets to its own speed: fixed terminals will use the lowest frequencies, while highly mobile terminals will send frequent updates.

4.3.2.4. Location-aided routing (LAR)

The LAR protocol [21, 22] is a typical on-demand routing protocol. In order to find a route between source and destination terminal, it relies on a flooding-based route discovery procedure originated by the source by means of a broadcast route request (RRQ) packet. The packet is forwarded by other nodes all over the network until either it reaches the destination (in which case the connection enters in the *found* status) or a timeout expires leading to a route discovery failure. When the destination receives an RRQ packet from the source, it replies with a route reply (RRP) packet which proceeds backward on the selected path, until it reaches the source, that can then start the transmission of data (DATA) packets. A node which detects a connection failure while sending or receiving RRP or DATA packets starts an alarm procedure based on the transmission of broadcast route reconstruction (RRC) packets. When an RRC packet reaches the source of the connection, the transmission of DATA packets is stopped, and the source decides either to drop the connection or to start searching for a new path to destination.

The major drawback of a flooding-based on-demand protocol is the huge amount of routing overhead generated during path search procedures. The location-aided routing exploits location information in order to reduce the amount of routing overhead, although in a different way from the DREAM algorithm described in Section 4.3.2.3. The LAR protocol uses in fact the location information during connection set-up in order to reduce the number of control

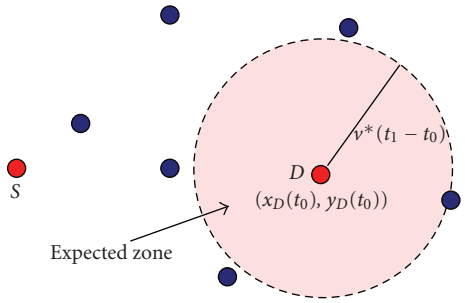

FIGURE 4.5. Definition of *expected zone* in the LAR protocol. If source S knows the position of destination D in $t = t_0$, $(x_D(t_0), y_D(t_0))$, and the maximum speed v of D, it can define the region in which D can lie within in $t = t_1$ (*expected zone*) as a circle of radius $d_{\text{MAX}} = v \cdot (t_1 - t_0)$ centered in the position of D in $t = t_0$.

packets, while no position information is used during DATA packets transmission, since they are sent along the path found during the set-up phase. The basic location information required by LAR consists in

(i) source position,
(ii) destination position,
(iii) maximum terminal speed.

Such information is exploited during the route discovery procedure as follows. Suppose that a terminal S starts a route discovery procedure to destination D at time $t = t_1$, and that the last information update regarding D's location was received by S at $t = t_0$. Based on the estimation of the maximum speed v of terminal D, S can evaluate the maximum distance traveled by D since the last location update. Such a distance is given by $d_{\text{MAX}} = v \cdot (t_1 - t_0)$. As a consequence, the current position occupied by D lies in a circular region of radius d_{MAX} centered on $(x_D(t_0), y_D(t_0))$, referred to as the *expected zone*, represented in Figure 4.5.

The expected zone indicates which zone of the network should be reached by RRQ packets. The key idea in LAR is to exploit this information to reduce the amount of RRQ packets flooding through the network, by allowing forwarding of packets generated by the source only in the direction of the expected zone containing the destination. The region of the network in which forwarding is allowed is referred to as *request zone*. An intermediate terminal is allowed to forward an RRQ packet only if it lies within the request zone defined by the source of the connection request.

Note that the request zone may be defined in several ways, the only constraint being that such zone must include both the position of the source S and the expected zone. A smaller request zone leads to a stronger reduction of the routing overhead, and can thus achieve a higher power efficiency; on the other hand, it leads to a lower number of neighbors involved in the route discovery procedure, and may cause a lower percentage of successful connections. Figures 4.6 and 4.7 show two different definitions of the request zone, and the effect on the number of neighbors involved in the route discovery procedure. In Figure 4.6 a conic request

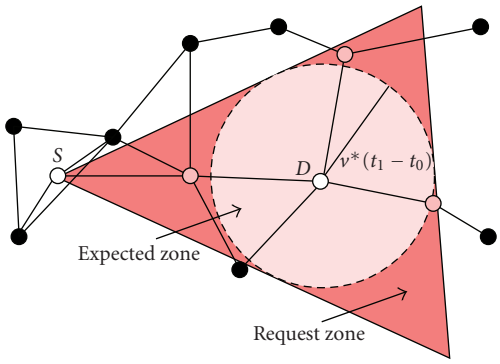

FIGURE 4.6. Definition of conic request zone in the LAR protocol. The nodes that fall within the request zone defined by source S and destination D are represented in grey, while the nodes that are not involved are represented in black.

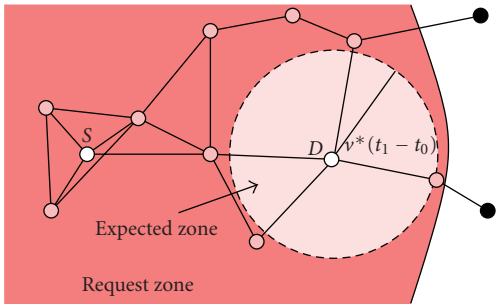

FIGURE 4.7. Definition of spherical request zone in the LAR protocol. The nodes that fall within the request zone defined by source S and destination D are represented in grey, while the nodes that are not involved are represented in black.

zone is considered, similar to the forwarding region defined in the DREAM protocol, while a spherical request zone is presented in Figure 4.7.

In both figures nodes that are involved in the route discovery procedure are represented in grey, while the nodes which are not involved are black. It is evident that the conic request zone reduces the overhead much more effectively than the spherical one, since a lower number of nodes forwards the RRQ packets. On the other hand, for particular topologies the conic request zone may lead to connection set-up failures which could be avoided with a larger request zone. An example of route discovery failure is shown in Figure 4.8, which shows a situation in which no intermediate nodes in physical connectivity with the source fall within the request zone.

The choice of size and shape of the request zone is thus the result of a trade-off between effectiveness in overhead reduction and probability of successful connection set-up.

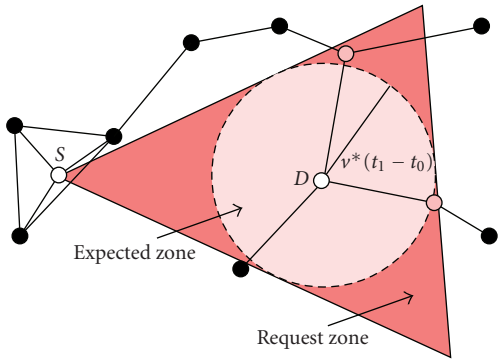

FIGURE 4.8. Route discovery failure due to a conic request zone in the LAR protocol. The nodes that fall within the request zone defined by source S and destination D are represented in grey, while the nodes that are not involved are represented in black. Note that a route discovery procedure generated in S and directed to destination D fails, since none of the grey nodes is in physical connectivity with the source S. A larger request Zone, involving black nodes, would instead lead to a success.

A more advanced trade-off can be obtained by allowing the source node to perform several attempts of route discovery to a given destination and adopting in each attempt an increasingly larger request zone: the result would be a higher percentage of successful connection set-ups, at the price of a higher overhead, obtained as the sum of the routing packets transmitted in each attempt.

This approach neglects, however, the effect on the latency in connection set-up: since each attempt would require a significant amount of time, the interval between connection request and set-up may turn out to be unacceptable in case of delay-sensitive applications.

As in the case of the DREAM protocol, information about the position of the destination is required at the source in order to reduce routing overhead, and thus location information must be disseminated through the network. Oppositely to DREAM, however, in LAR such dissemination is performed by piggybacking location information in all routing packets, without any additional control packet. At the beginning of network operations, terminals will be thus forced to find routes in the absence of location information. In such a situation basic flooding is adopted.

4.3.3. From GPS to UWB positioning

The protocols described in Section 4.3.2 share the common assumption that each terminal retrieves its own location information from GPS. As a consequence, protocols focus on how to disseminate location information, assuming the problem of retrieving it as solved.

The adoption of the UWB technology in place of GPS as the basis for retrieving position information opens new doors to location-based applications (such as indoor deployment), but also poses new challenges.

Since UWB can only provide ranging information, in fact, distributed processing of ranging measurements is required in order to build a network map. The problem of how to build such a map is not trivial, in particular in the case of a pure ad hoc network, where no fixed reference points are available. The self-positioning algorithm (SPA) [23], proposes a solution to this problem. The SPA is composed of two steps. First, each node in the network attempts to build a coordinate system centered on itself, and to determine the position of its neighbors in this system. Second, the node-centered coordinate systems converge to a global network-wide coordinate system.

In the first phase, each node N_i tries to build a coordinate system by

(1) detecting the set of its one-hop neighbors K_{N_i}, by using beacons,
(2) evaluating the set of distances from its neighbors D_{N_i},
(3) broadcasting D_{N_i} and K_{N_i} to its one-hop neighbors.

Since all nodes perform the above procedure, node N_i knows the distance from all its one-hop neighbors, the IDs of its two-hop neighbors, and a subset of the distances between the one-hop neighbors and the two-hop neighbors. This information is used by N_i to build its own coordinate system.

In the second phase, all coordinate systems evolve into a network-wide coordinate system by choosing the same orientation of the x and y axes. Iteratively, pairs of nodes rotate and align their coordinate systems. Using this distributed approach, a network-wide coordinate system is eventually achieved. Note that nodes that are not able to build their own node-centered coordinate system can obtain their position in the network-wide coordinate system if they are in range with three nodes that already received the coordinate system.

UWB-based positioning poses thus additional requirements, with respect to GPS, to location-aided routing protocols.

(i) Determination of a network-wide coordinate system may require a long time. Furthermore, occasional large errors in position information due to lack of connectivity or unfavorable topology may occur. The routing algorithm must be then capable to find routes and establish connection even for incomplete or lacking positioning information.
(ii) Estimation of absolute terminal speeds is in general not available.

The GPSR protocol requires a location service in order to provide the position of the destination to the source, in order to mark the packet with such information. When this location service is not available from start, as in UWB-based positioning, each data packet must be forwarded by means of flooding, with a high routing overhead.

LLR can be adapted to a UWB-based positioning system with minor changes, but the protocol is inherently tailored for scenarios characterized by terminal mobility (in which route stability is the main concern), and does not offer major advantages in terms of power efficiency in networks composed of still or slowly mobile terminals.

In the DREAM protocol, both selection of routes and dissemination of information rely on positioning to work properly: in particular, the proactive dissemination algorithm exploits the capability of a terminal to determine its physical

distance from terminals which are not reachable, to evaluate the validity of an update packet. If location information is not available or subject to errors, both the proactive and reactive parts of the protocol are affected. Furthermore, lack of speed information poses an additional issue to the correct behavior of the protocol.

Oppositely, LAR protocol inherently offers a backup solution when no positioning information is available. In fact, in the case of absence of information regarding the position of the destination, the protocol switches to a basic flooding scheme, resembling a dynamic source routing [24] protocol. In this case the lack of positioning information results in a reduced efficiency of the protocol.

The above considerations led to the choice of adopting LAR as the routing protocol for the integrated power-efficient and location-aware solution presented in the next section.

4.4. Power-efficient and location-aware medium access control design

4.4.1. Introduction

The analysis carried out in Sections 4.2 and 4.3 showed that both distance and position information can be exploited in order to optimize network performance by reducing power consumption and enabling location-aware path selection strategies. In the case of UWB networks, in particular, it was highlighted in Section 4.3 that position information must be derived by means of a dedicated protocol from distance information. The design of a medium access control protocol capable of providing accurate distance information is thus a fundamental step for the development of advanced location-aware strategies in UWB networks.

In this section we will introduce a MAC protocol which foresees a dedicated procedure for the acquisition of distance information, and is furthermore tailored for the characteristics of UWB in a low data rate application scenario: the so-called uncoordinated, wireless, baseborn medium access for UWB communication networks $(\text{UWB})^2$.

4.4.2. The $(\text{UWB})^2$ MAC protocol

As already mentioned in Section 4.2, CSMA is almost universally adopted in MAC for narrowband wireless networks, since it overcomes the drawback of frequent packet collisions experienced in the case of plain Aloha [25]. The CSMA approach, however, shows significant advantages over the Aloha approach under the two following key hypotheses:

(1) simultaneous transmissions of multiple packets result in destructive collisions because of multiuser interference,
(2) high traffic is offered to the network.

Although the above hypotheses are reasonable in a traditional narrowband wireless LAN, we will discuss in the following why this may not longer be the case for a UWB network, in particular when low data rate applications, such as those typical of sensor networks, are considered.

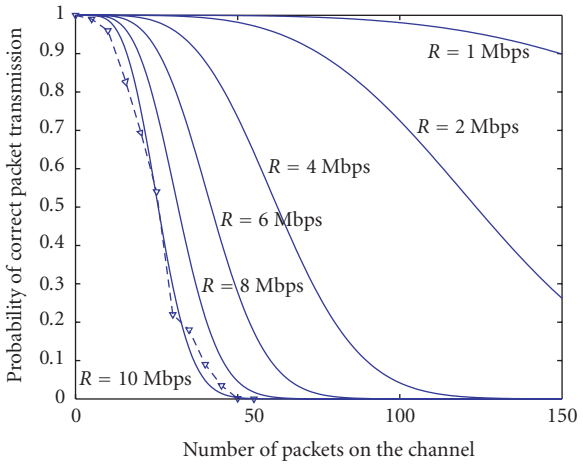

FIGURE 4.9. Probability of successful packet transmission as a function of the number of packets on the channel. Different solid lines correspond to different data rates from 1–10 Mbps. The dashed line shows simulation results in the specific case of $R = 10$ Mbps. Drawn from [26].

We will refer throughout this analysis to the specific case of time-hopping impulse radio UWB (TH-IR-UWB), for which the $(\text{UWB})^2$ was originally designed. The applicability of the ideas exposed here to other UWB variants, such as direct sequence UWB or multiband OFDM UWB remains to be analyzed.

As explained in previous chapters, UWB in its impulse radio version is based on the emission of very short pulses which are modulated in position (pulse position modulation (PPM)) or amplitude (pulse amplitude modulation (PAM)) by the information bits. The duty cycle of emitted signals depends thus on the ratio between the pulse repetition period (PRP), that is, the average interval between two consecutive pulses, and the duration of a pulse. In the case of low data rate transmissions, where bit rates in the order of 100 kbps, or below, can be considered as an acceptable target, this corresponds to signal duty cycles as low as 10^{-6}: the adoption of short pulses offers thus an intrinsic protection from MUI.

Simulation results presented in [26] suggest in fact that in the case of LDR scenarios, the huge bandwidth adopted for transmissions translates in very short, rare pulses, and thus in a low probability of collisions between pulses emitted by different terminals. Under this condition the probability of packet error is negligible even in presence of 100 simultaneous packet transmissions (see Figure 4.9, drawn from [26]).

In the case of PPM, the UWB signal is quasiperiodic due to the rather small PPM shift value which is usually adopted. In order to mitigate energy peaks at multiples of the average pulse repetition frequency, time intervals between UWB pulses must be randomized. This is achieved by adopting TH codes, which introduce additional pseudorandom delays in pulse transmissions. The adoption of the TH principle also offers an additional degree of freedom for multiple access, which

can be obtained by assigning different TH codes to different users, thus adopting a TH code division multiple access (TH-CDMA) scheme.

The above considerations led to the definition of the $(UWB)^2$ protocol.

$(UWB)^2$ is a multichannel MAC protocol. Multichannel CDMA MAC algorithms, commonly referred to as multicode, have been intensively investigated for direct sequence (DS) CDMA networks [27–29]. Note, however, that although in the last years most of the research efforts were focused on DS CDMA, frequency hopping (FH) CDMA and TH-CDMA also provide viable solutions.

The $(UWB)^2$ protocol applies indeed the multicode concept to the specific case of a TH-IR UWB system. $(UWB)^2$ adopts a hybrid scheme based on the combination of a common control channel, provided by a common TH code, with dedicated data channels associated to transmitter TH codes. The adoption of a hybrid scheme can be motivated as follows:

(1) it simplifies the receiver structure, since data transmissions (and corresponding TH codes) are first communicated on the control channel;
(2) it provides a common channel for broadcasting. This is a key property for the operation of protocols in higher layers. Broadcast messages are, for example, required for routing and distributed positioning protocols.

As regards code assignment, a unique association between MAC ID and Transmitter Code can be obtained by adopting the algorithm described in [30] which avoids implementing a distributed code assignment protocol.

The multiple access capability warranted by the TH codes is used by the $(UWB)^2$ protocol in data transmission. The protocol relies for the access to the common channel on the high MUI robustness provided by the processing gain of UWB.

$(UWB)^2$ is designed for distributed networks dedicated to low data rate applications. As a consequence, it does not assume that synchronization between transmitter and receiver is available at the beginning of packet transmission, because of clock drifts in each terminal during inactivity periods. As a consequence, a synchronization trailer long enough to guarantee the requested synchronization probability is added to each packet. The length of the trailer depends on current network conditions, and is provided to the MAC by the synchronization logic.

In the view of allowing the introduction of the location-related functions presented in the previous sections, in particular distributed positioning and location-aware routing, $(UWB)^2$ also exploits the ranging capability offered by UWB. Distance information between transmitter and receiver is in fact collected during control packets exchange.

The procedures adopted in $(UWB)^2$ for transmitting and receiving packets, described in [26], have in fact two main objectives:

(i) to exchange information such as the adopted synchronization trailer, that is, hopping sequence and length,
(ii) to perform ranging. Since no common time reference is available, a two-way handshake is required to collect distance information by estimating the round-trip time of signals in the air.

An example of such procedure is shown in Figure 4.10, where a transmitter Tx and

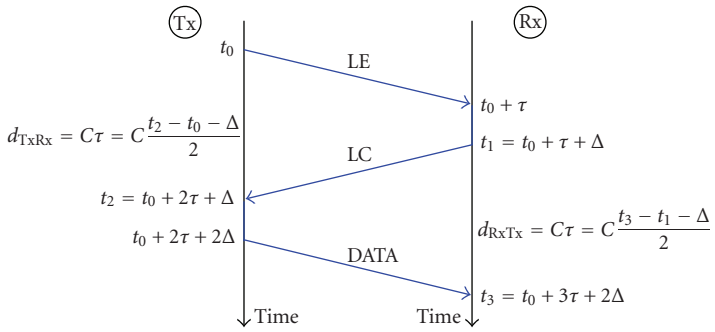

FIGURE 4.10. Example of two-way ranging procedure.

receiver Rx set up a DATA packet transmission by exchanging a link establishment (LE) packet transmitted on the common code, followed by a link confirm (LC) packet transmitted on the transmitter code of the receiver Rx, and finally by the DATA packet on the transmitter code of transmitter Tx. Thanks to the adoption of a delay Δ known to both Tx and Rx, this handshake allows the determination of the propagation delay τ and thus of the distance Tx–Rx to both the devices involved in the communication.

The ranging procedure made available by $(\mathrm{UWB})^2$ provides the information that is required by the positioning and routing algorithms, and thus enables the adoption of a location-aware, power-efficient path selection strategy, based on the combination of three key components: the $(\mathrm{UWB})^2$ MAC protocol [26], the self-positioning algorithm [23], and the location-aided routing protocol [21].

Performance analysis of such strategy in specific test cases, characterized by different degrees of mobility and different mobility models, will be the subject of the next section.

4.5. Performance analysis in specific test cases

4.5.1. Introduction

In this section we will analyze the performance of the solution presented in the three previous sections of this chapter, composed of the $(\mathrm{UWB})^2$ MAC protocol, of a distributed positioning protocol, and of the LAR routing protocol, combined with a power-aware routing metric. The analysis will focus on two main aspects:

(i) effectiveness of the proposed solution in terms of network lifetime and throughput,

(ii) effect of mobility on system performance.

To this aim, we first address the problem of mobility modeling, by comparing several mobility models and determining their effect on network topology. Next, we define three test cases, each of them with different node mobility characteristics. The behavior of the proposed MAC and routing strategy within each test case is finally studied.

4.5.2. Mobility models

Introducing mobility within the simulated scenarios allows to test the proposed protocols under more realistic conditions. This is particularly true for routing protocols, where performance greatly varies with the topology of the network. Since different mobility models lead to different topologies, however, it is important to select the mobility model that best fits the reference scenario, that is, the typical mobile user that each node in the network represents.

Different mobility models are presented in literature. An interesting subclass is composed by *group* mobility models. This class of models was introduced to emulate particular node behaviors, such as crowds moving towards a common destination or rescue (and similar) squads, where each node is bound to show some degree of mobility similarity with other nodes belonging to the same group.

4.5.2.1. Mobility models in literature

Several mobility models for ad hoc network are proposed in the literature: (1) the Random Mobility or Brownian model [31], with no relation between speed and direction of the node in two subsequent timeslots; (2) the Random Direction model [32], with nodes keeping the same velocity during the whole simulation; (3) the Ko mobility model used for evaluating the LAR protocol [21], according to which the path walked by the node is formed by sections with exponentially distributed length and random direction; (4) the Markovian model [33], which has many moving states and a transit matrix used to determine whether the node should keep or change the current motion direction; (5) the Random Waypoints [24], whose movement paths are composed of segments with random speed, direction, and duration, separated by stand-still periods, simulating pausing intervals; (6) the Inertia [34], in which the node moves along a random direction, with random speed, for a random time, and then decides whether to keep the same movement characteristic for the next movement segment (the node's inertia), or to select a new direction, speed, and duration.

All the previous models are, clearly, inadequate to simulate a group movement, since each node has its own movement pattern, which has no relationship with those exhibited by other nodes; in fact, these models were mainly developed with the aim of testing traffic loads offered to the system, rather than reproducing realistic behaviors.

The need for group mobility models, showing correlated movements among the nodes and offering flexibility for the implementation of particular behaviors, has lead to the design of other models; among these, the exponential correlated random (ECR) model [35]. Other approaches are proposed in literature, in order to bypass the limitation of ECR; those reviewed here are the Reference Point Group Mobility model [36], and the Reference Velocity Group Mobility model [37]; besides these models, a new proposal, the Kerberos mobility model, has been designed and is presented in this section.

An important note on the choice of the mobility model is that, besides models designed with other aims, there exist no "good" or "bad" mobility models: each

model is different. Each mobility model may or may not show a global, mobility-related property, that could in turn be exploited by the system. The capability of taking into account the characteristics of the mobility model during the design phase marks, therefore, the difference among a general/unoptimized system, and a well-designed one.

4.5.2.2. Nongroup mobility models

In order to make a comparison between group and nongroup mobility models, simulations were performed, which adopt two nongroup mobility models: the Random Waypoints [24], and the Inertia [34] models.

In the Random Waypoints model, each node selects a random direction, speed, and movement duration; at the end of the movement, the node stands still for a random time; after the pause time, the node selects a new random direction, speed, and movement duration, and starts walking along the new path. The Random Waypoints model shares a particular mobility pattern with other models adopting the random direction approach: the "density wave" effect, with a greater concentration of the nodes in the central area.

According to the Inertia model, after the end of its movement segment, a node must choose the direction for the next segment. The two alternative choices for the next segment are: (1) the node keeps the current direction, with probability ρ, or (2) the node selects randomly a new direction, with probability $1 - \rho$; the weight of the two alternatives can be different, with a higher probability of keeping the current direction ($\rho > 1/2$). The name Inertia refers indeed to the node property of seldomly changing its direction.

4.5.2.3. Group mobility models

Group mobility models, as previously stated, require that nodes movements are, somehow, related. In particular, two kinds of relations can be imposed on the nodes: (1) the nodes must show some relationship in their directions and/or velocities, or (2) the nodes must be somehow close to each other. Models of the first kind are better suited to simulate the movement of a crowd heading towards a given direction; such models show the *network partition* property, with nodes of a given group emerging by the compound of all network nodes and forming, in vast areas, distinguishable subnetworks of nodes with similar velocities and directions. When, on the contrary, the relationship among group nodes is a distance one, the resulting geographical distribution is characterized by the concentration of the nodes in a limited area; in this case, the nodes usually do not show any relationship in velocity or direction.

Reference point group mobility. The Reference Point Group Mobility (RPGM) model was developed by Hong et al. in [36]. To represent the group mobility behavior of the mobile nodes, the model defines, for each group, a logical *reference point*, whose movement is followed by all nodes in the group. The path the reference point moves along defines the entire group mobility behavior, including

location, speed, direction, acceleration, and so forth. Thus the group trajectory is determined by providing a path for the reference point, with any node in the group randomly placed in the neighborhood of its reference point.

Once next position (x, y) of the reference point is determined (the path of the reference point can be selected with any nongroup-oriented mobility model), each other node position is calculated adding a random motion vector $\overrightarrow{\mathrm{RM}}$ to (x, y). The length and direction of this module can be determined through any policy; the authors of the model suggest a uniform distribution within a given range from the reference point for the length, and a uniform distribution between 0° and 360° for the direction.

Main RPGM characteristic is that the groups are characterized by *physical proximity*, that is, all the nodes are close to the reference point. Obviously, the way this physical proximity translates itself into actual distribution of the nodes within deployment area depends on the values actually used for the distribution of the length of the $\overrightarrow{\mathrm{RM}}$ random motion vector.

One drawback of the direct implementation of such a mobility model is that it does not implement a check on the maximum/minimum node velocity, because of the position-based approach. Since the resulting position of a node is calculated as the sum of two vectors, the reference point position (x, y) and the random motion vector $\overrightarrow{\mathrm{RM}}$, it is possible, for given values of these two parameters, that the node should have a speed higher than its maximum; a similar case holds for the minimum velocity.

About the resultant distribution of the nodes, the adoption of this approach typically distributes the nodes inside a circular area centered around the reference point: the wider the distance from the reference point, the more vast the area in which the nodes are distributed, the looser the bonds between the nodes in the group.

Reference velocity group mobility. The Reference Velocity Group Mobility (RVGM) model has been presented in [37] as an evolution of RPGM. The fundamental concept proposed is that movement similarity is a more fundamental characteristic for group mobility than physical proximity; thus nodes being part of the same group should show close velocities and directions, rather than physical proximity.

Each group, therefore, is characterized by a *group velocity*. The nodes that are members of the group have velocities close to the characteristic group velocity, with slight deviations. Hence, the characteristic group velocity is also the mean group velocity. The distributions of both the group velocity and the velocity deviation can be of any type, in order to model the various possible mobility patterns.

Main characteristic for RVGM is that, in a scenario with infinite dimensions area, the network will eventually incur a complete partition, with each subnetwork corresponding to a group; in a finite-dimensions area this behavior is not fully developed, because of the presence of area boundaries, but is latently present in the movement patterns.

The main reason why RVGM was evolved from RPGM is that the former model is better suited when dealing with mobility or partition prediction purposes; representing the nodes by their physical coordinates, RPGM does not allow to easily detect group movement patterns and the trend in network topology changes.

About the resultant distribution of the nodes, the adoption of this approach typically distributes the nodes to cover the whole area with nodes with similar velocities and directions.

Kerberos mobility model. The basic concept in Kerberos mobility model is that each node in a group is allowed to move around freely, provided it keeps contact with the other nodes in its group.

This basic concept can be translated into the adoption of a condition of physical proximity between the given node and the other nodes of its group: when this condition is met, the node moves according to a nongroup mobility model (e.g., Inertia), while, when the node is far from its fellows, it is obliged to move closer to them.

The difference between *Kerberos* and RPGM models is that, in the latter, each node follows the reference point and, for this reason, is close to its fellows; this is how physical proximity arises in RPGM. In the *Kerberos* model, on the contrary, it is explicitly required for each node to monitor its distance from its fellows, and to stay close to them.

Kerberos requires that, after each mobility update, each node checks how many nodes of its own group it is connected to: this set of nodes forms the *fellowship* of the node. Two nodes in the same fellowship can be connected through a direct link when the destination node is within range, or through relaying of intermediate nodes, all belonging to the group, which are at the same time, members of the fellowship. If the number of nodes in the fellowship is greater than half the number of nodes forming the group, the node is allowed to move freely; otherwise, the node is separated by the main chunk of group (if any exists), and is compelled to move towards the closest group node not belonging to its fellowship.

Notes on group mobility models. The different approaches adopted by RPGM, RVGM, and *Kerberos*, are characterized by different and characterizing patterns in the disposition of the nodes belonging to a single group. In the case of RPGM, since the nodes are bound to stay within a given range from the same point, each group forms a globular pattern, centered around the reference point; this usually means a high level of connectivity between the nodes in the group. On the other hand, in the case of Kerberos, there are higher probabilities for patterns in which the nodes form a chain or a line; this happens because, once connectivity requirements are verified, each node is allowed to move freely, and therefore even further from the group itself.

However, *Kerberos* mobility model is closer to RPGM than to RVGM; it is possible, changing the connectivity requirement into a maximum distance from a chosen node (the "group leader"), to obtain mobility patterns very similar to RPGM.

4.5.2.4. Mobility model metrics and test scenario

In order to analyze the impact of different mobility models on the performance of a routing protocol, it is appropriate to simulate the mobile network and to test the protocol. It is also possible, however, to analyze the topological characteristics of networks adopting the different mobile models. These topological properties have, obviously, a deep impact on routing performance: for example, the average number of nodes within range will affect the route availability between any two given nodes, so that those mobility models that scatter the nodes over the whole simulation area are expected to have a lower route availability than those mobility models which concentrate the nodes in smaller areas.

In [38], the authors provide a number of mobility model metrics, to be applied to the evaluation of mobility models impact on routing performance.

(i) *Number of link changes*: the number of transitions from the state "connected" to the state "disconnected" and vice versa, for the link between any pair of nodes in the network. Its average over the number of links in the network is the *average number of link changes*, and is calculated separately for links between nodes of the same group and for links between nodes of different groups.

(ii) *Link duration*: the average duration of the link between two nodes, that is, the average time that two nodes remain continuously within range. Its average over the number of links in the network is the *average link duration*, and is calculated separately for links between nodes of the same group and for links between nodes of different groups.

(iii) *Path availability*: the fraction of time during which a path of links within transmission range is present between two nodes in the network. Its average over the number of links in the network is the *average path availability*, and is calculated separately for paths between nodes of the same group and for paths between nodes of different groups.

We propose an additional metric, in order to evaluate the probability that any two given nodes are within range.

(iv) *Link availability*: the percentage of time during which link between two given nodes is active, that is, the two links are within transmission range. Its average over the number of links in the network is the *average link availability*, and is calculated separately for links between nodes of the same group and for links between nodes of different groups.

The simulation scenario consisted in a network of 16 nodes, divided into 4 groups of 4 nodes each. The deployment area was a square with 100 m sides, with transmission range equal to 20 m. The simulations have been performed with different values for node maximum velocity, from 1 m/s to 10 m/s, and lasted 2 hours. As regards the mobility model parameters, RPGM $\overrightarrow{\text{RM}}$ maximum length has been set to 30 m; *Kerberos* simulations were performed adopting Inertia as mobility model when a node is free to move.

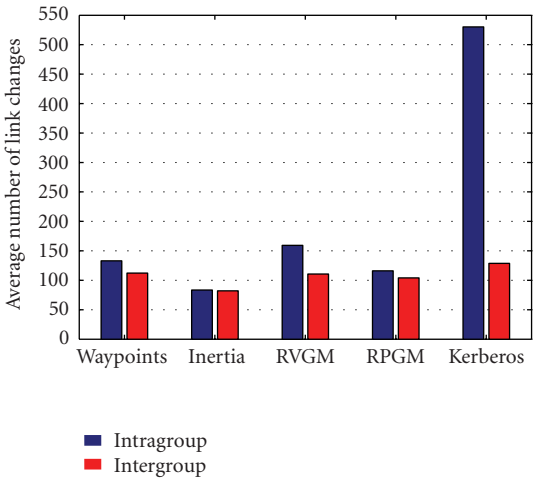

FIGURE 4.11. Average number of link changes for different mobility models.

4.5.2.5. Mobility models simulation results

Number of link changes. Figure 4.11 shows the average number of link changes for all the mobility models investigated, and for both intergroup and intragroup cases; the values are expressed in average number of changes per minute.

Kerberos shows a high number of changes in links between nodes belonging to the same group. This is the result of two behaviors:

(i) when a node is connected to the group, it is allowed to move freely, without any constraint based on the positions of the other nodes of its group. This means that nodes in the same, connected, group may be headed along different directions; the result is a high number of link breaks or set-ups;

(ii) when a node detects that its group is disconnected, it is compelled to move towards the other nodes in its group: the result is the set-up of one or more links with group nodes.

The second most notable result in Figure 4.11 is that the difference between intra and intergroup links is higher in group mobility models than in nongroup ones: a foreseeable effect of the group bound observed by the former models, since the latter do not make distinction between group and nongroup mobility models.

In the evaluation of a routing protocol, this mobility model metrics can give an estimation of the control traffic that the protocol produces each time a link is established or is broken: this includes control traffic to update network topology knowledge, alternative route checking, and so forth.

Link duration. The average link duration of each mobility model is shown in Figure 4.12, for intra and intergroup links; the values are expressed in seconds.

This mobility model metrics tells apart the group by the nongroup mobility models: the former show a high difference in average link duration between intra

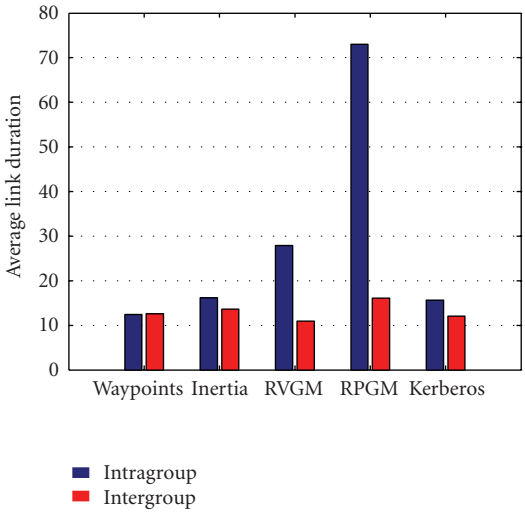

FIGURE 4.12. Average link duration, in seconds, for different mobility models.

and intergroup links. In the case of RVGM, the higher duration for intragroup links is derived from the circumstance that, if two nodes form an intragroup link, they have a large probability to have similar velocities and directions. In the case of *Kerberos* and, above all, RPGM, the *physical proximity* property is what make the link more stable: the nodes forming the intragroup link are very likely to remain close in the future. *Kerberos* shows the lowest average link duration among group mobility models, because group nodes neither share similar velocities and directions (as in RVGM), nor are compelled to stay within a maximum distance from a common point; however, the constraint on group connectivity allows a node to break its intragroup link only if it has, at least, another intragroup link, otherwise it will depart from its group. Between the nongroup mobility models, Inertia has a slightly higher average link duration than Random Waypoints. This is due to the fact that the two nodes composing the link will be more likely to keep on moving in the same direction if they are modeled with Inertia, rather than with Random Waypoints.

This metric shows different information, with respect to the *number of link changes*, because it measures the length of a connection *after* it has been established, while the other metric measures the frequency of link establishment. Taking RPGM and Random Waypoints as examples, these models have *average number of link changes* values that are very close, but their values for *average link duration* are far apart: this happens because both establish links with the same frequency, but those exhibited by RPGM are built by nodes that are compelled to stay close for a long time, while in Random Waypoints the nodes usually break the link shortly after they build it.

Regarding routing, this metric gives an estimation of the average reliability of a link. This parameter impacts the procedures that must select the most reliable

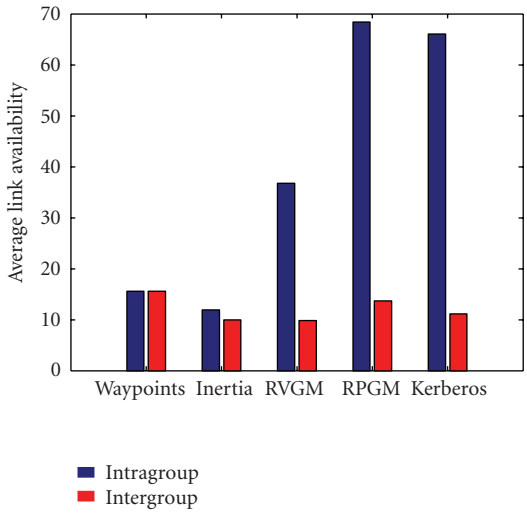

FIGURE 4.13. Average link availability, in percentage of time, for different mobility models.

route among several possible: it is clear that a route mainly composed of intragroup links will be much more reliable than another mainly composed of intergroup links—under the hypothesis of the adoption of a group mobility model.

Link availability. Figure 4.13 shows the results for the *average link availability* metric, expressed in percentage of time in which a given link is established.

It is clear how group and nongroup mobility models greatly differentiate themselves, as regards the availability of a link. Nongroup mobility models do not distinguish between intra and intergroup links; also, the percentage of availability of a link is quite low, since the link is formed by nodes that move in a completely independent fashion. Group mobility models, on the contrary, highly privilege intragroup links over the others: the similarity in the movement of the RVGM, the physical proximity requirement of the RPGM, and the group connectivity constraint of Kerberos, all result in a more probable presence of a link between nodes of the same group; on the other side, nodes from different groups are compelled to have different movement behaviors, ending in less frequent links.

Through the average link availability mobility model metrics, it is possible to determine the expected number of links a node has. The connectivity of a node is an important parameter for a routing protocol: it can be used to calculate the expected load on each link, to estimate the capability of performing relaying for other nodes traffic.

Path availability. Simulation results for the average path availability are shown in Figure 4.14. For each possible pair of nodes in the network, simulations have been performed to determine the probability of existence of a path, composed of one or more links. The intragroup paths are those in which the starting and the ending nodes of the path are members of the same group.

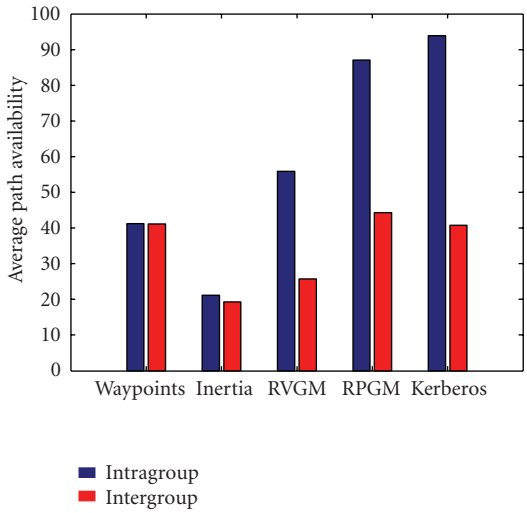

FIGURE 4.14. Average path availability, in percentage of paths, for different mobility models.

Once again, it is possible to tell apart the group from the nongroup mobility models, because of the difference between inter and intragroup values, and of the value of the latter case. As expected, nongroup mobility models show no difference between intra and intergroup paths, since all the nodes are moved independently from their group fellows. The difference between Random Waypoints and Inertia is given by the fact that Random Waypoints scatters the nodes all over the simulation area: the probability of network partition (which implies a dramatic decrease in average path availability values) is therefore high, but is lower than in Inertia, where some nodes tend to be separated by the remaining network for long times. As regards the group mobility models, note that

(i) *Kerberos* shows the highest average path availability for intragroup paths. With the adoption of this mobility model, the network shows highly connected groups that span over wide areas. intragroup links are less frequent, but they allow a large number of paths to exist;

(ii) RPGM shows a lower *average path availability* for intragroup paths, but higher than *Kerberos* for intergroup ones. Physical proximity requirement allows for a few group partitions, but the groups cover wider areas than *Kerberos*, thus increasing the probability of an intergroup link, which sustains a number of intergroup paths;

(iii) RVGM results are due to the aforementioned property of similarity in movements, rather than in physical proximity, for the nodes of a group. The resulting values are similar to an average between the nongroup and the remaining group mobility models.

As one could expect, the *path availability* mobility model metrics is the one with the most direct impact on routing performance. It, in fact, directly translates in the probability of existence of a path between any two given nodes. Low path

probabilities could require routing strategies that invest few resources in path discovery, since there is a higher possibility that this procedure ends in a failure.

Simulation results show that different mobility models have quite different properties, as regards the *path availability*: comparing, for example, the Random Waypoints and the RVGM, the latter shows a higher availability for intragroup path than the former, while the opposite holds for intergroup paths. The actual answer on the global path availability depends on the ratio between intra and intergroup links in the actual network, that is, on the ratio between group and network cardinality. It is important to underline, however, that in those scenarios in which group mobility models are more suited, there is, typically, also a traffic relationship between group nodes; that is to say, a node will be more likely to communicate with nodes of the same group, rather than nodes of other groups: the effect of this property is that the actual percentage of routes found depends also on the ratio between intra and intergroup path, weighted with the ratio between intra and intergroup communications.

4.5.3. Test cases

We will investigate three different test cases which are characterized by the following common scenario: a network of N terminals deployed in initial random positions. Each terminal periodically generates a connection request to a random destination, following a Poisson distribution with average time λ between two subsequent requests. Each connection request is characterized by a constant bit rate R_c and a total number of bits to be transferred which is randomly selected in the interval [1, MaxDimBit]. Each terminal is furthermore characterized by a total amount of energy E_{TOT}, which is reduced after each packet transmission or reception based on the following energy model [39]:

$$\begin{aligned} E_{\text{TX}} &= E_{\text{start}} + L \cdot \left(E_{\text{Tx-bit-rate}}(R_b) + E_{\text{Tx-bit-prop}}(R_b) \cdot d^{\alpha}\right), \\ E_{\text{RX}} &= E - \text{start} + L \cdot \left(E_{\text{Rx-bit-fixed}} + E_{\text{Rx-bit-rate}}(R_b)\right), \end{aligned} \tag{4.8}$$

where L is the length of the packet.

Note that, although this model is not specific for UWB, it addresses a class of devices which is close, in terms of achieved bit rate and complexity, to the UWB devices foreseen for low bit rate networks.

All test cases share furthermore the settings adopted for positioning and routing protocols, in particular data and control packet sizes. Finally, the initial amount of energy E_{TOT} for each node is the same in all the three test cases, although its actual value depends on the transmission range.

The three test cases differ however in the mobility pattern of the terminals.

(i) Test case 1: network of still terminals in random positions.

(ii) Test case 2: network of mobile terminals in initial random positions, following the *inertia* mobility model.

(iii) Test case 3: network of mobile terminals in initial random positions, following the *Kerberos* mobility model.

The initial selection of terminal positions can heavily influence the network performance, in particular in the scenario considered in test case 1: as a consequence, in order to determine the average performance of the strategies, N_{runs} simulation runs were executed, with terminals deployed in random positions in an area of A_{side}xA_{side} m^2. Given a set of terminals in random coordinates, however, network topology is also determined by the transmission range, which influences the network connectivity. For this reason, tests were executed for three different transmission ranges, $R_{\text{TX-low}}$, $R_{\text{TX-med}}$, and $R_{\text{TX-high}}$, leading to low, medium, and high network connectivity, respectively. The common settings to all tests cases are presented in Table 4.1, while Table 4.2 presents the initial energy per node for each transmission range.

In each test case four different strategies were compared, which combine in different ways the two key components of the proposed solution: location-aided routing algorithm and power-aware routing metric. The distinction between the routing protocol and the routing metric allows in fact to evaluate the effect of each of the two components on system performance.

The four strategies are as follows:

(i) dynamic source routing with hop minimization (DSR + hop),
(ii) dynamic source routing with cost function minimization (DSR + cost),
(iii) location-aided routing with hop minimization (LAR + hop),
(iv) location-aided routing with cost minimization (LAR + cost).

As previously stated, the performance of each strategy was analyzed under conditions of limited available energy taking into account two aspects: long-term system performance, that is, how long the network is alive and thus capable of transferring data, and short-term system performance, that is, how network behaves during its life. The following routing strategy metrics were selected to measure long-term and short-term performance.

(i) Number of found connections.
(ii) Number of DATA packets delivered to destination.
(iii) Percentage of found connections.
(iv) End-to-end throughput for DATA packets.

A found connection is defined as a connection in which the destination terminal, following the reception of a routerequest (RRQ) packet, is able to send back to the source terminal a routereply (RRP) packet. The total number of found connections is a good indicator of the long-term behavior of the network since, given the constant rate λ of connection requests generation, a longer network lifetime will lead to a higher number of requested Connections and, eventually, of found connections. Since each connection, however, is set up in order to transfer DATA packets, we also consider the total number of DATA packets transferred during network lifetime, in order to determine which is the impact of each strategy at packet level.

The percentage of found connections, oppositely, allows to measure the network behavior in the short-term, by measuring how good each connection is served

Table 4.1. Simulation settings common to all test cases.

Parameter	Value
R_b	1 Mbps
R_c	50 kbps
λ	50 s
MaxDimBit	1 Mbit
N	20
α	4
E_{start}	$2.76 \cdot 10^{-5}$ J
$E_{\text{Tx-bit-rate}}$	$3.25 \cdot 10^{-7}$ J
$E_{\text{Tx-bit-prop}}$	$1.25 \cdot 10^{-11}$ J
$E_{\text{Rx-bit-fixed}}$	$1.13 \cdot 10^{-7}$ J
$E_{\text{Rx-bit-rate}}$	$2.79 \cdot 10^{-7}$ J
A_{dim}	80 m
$R_{\text{TX-low}}$	20 m
$R_{\text{TX-med}}$	40 m
$R_{\text{TX-high}}$	60 m
RRQ size	760 bit
RRP size	760 bit
DATA size	5000 bit
ACKDATA size	250 bit
RRC size	250 bit

by the network. The end-to-end throughput for DATA packets provides the same kind of short-term information at the packet level.

Note that the evaluation of the short-term performance behavior is fundamental in the comparison of the different strategies since, from a theoretical viewpoint, a strategy could lead to an overall high number of found connections, thanks to a long lifetime which allows for a high number of requested connections, but at the price of a low percentage of found connections.

4.5.3.1. Test case 1

This test case analyzed a scenario with terminals in fixed locations, which are unknown at start of operations.

Since terminals could not move, network topology only changed when a terminal ran out of energy: as a consequence, in this scenario, performance was significantly affected by the transmission range. Furthermore, as we will see, different strategies were affected in a different way by variations in network connectivity.

Figure 4.15 presents the number of found connections under conditions of low network connectivity. The LAR + hops strategy achieves the highest number of found connections, but the performance of the four strategies is quite similar, since the main factor in determining network behavior is the degree of network connectivity. This conclusion is also supported by the other indicators, that is, the

TABLE 4.2. Initial energy amount per node for each of the three transmission ranges considered in simulations.

Range	Energy E_{TOT}
$R_{\text{TX-low}}$	25 J
$R_{\text{TX-med}}$	250 J
$R_{\text{TX-high}}$	800 J

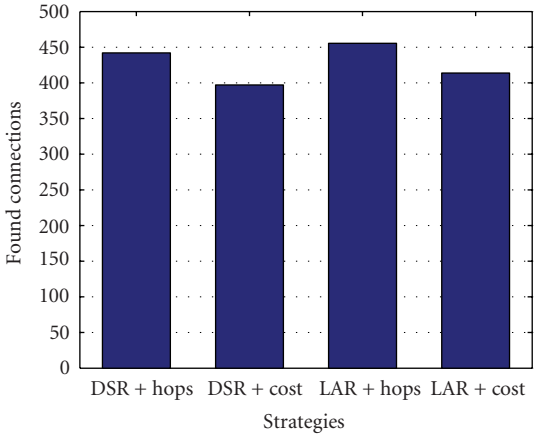

FIGURE 4.15. Found connections for test case 1 with $R_{\text{TX-low}}$.

number of DATA packets, the percentage of found connections, and the DATA throughput, presented in Figures 4.16, 4.17, and 4.18.

Interestingly, the adoption of the power-aware cost function in place of number of hops leads to slightly worse performance in terms of number of found connections and of delivered DATA packets, indicating a shorter network lifetime. This can be explained by observing that when the transmission range is low, the energy costs in transmission and reception which are not related to propagation are more relevant in the overall energy consumption, thus eliminating the advantage of increasing the number of hops per connection. As an example, let us consider the case of the transmission of a DATA packet over a distance $d = 10$ m. The overall energy cost of the transmission ($E_{\text{TX}} + E_{\text{RX}}$), based on the model in (4.8) is given by

$$\begin{aligned} E &= 2 \cdot E_{\text{start}} + L \cdot \left(E_{\text{Rx-bit-fixed}} + E_{\text{Rx-bit-rate}}(R_b) + E_{\text{Tx-bit-rate}}(R_b)\right) \\ &\quad + L \cdot \left(E_{\text{Tx-bit-prop}}(R_b) \cdot d^{\alpha}\right) \\ &= 5.52 \cdot 10^{-5} + 5000 \cdot \left(7.17 \cdot 10^{-7}\right) + 5000 \cdot \left(1.25 \cdot 10^{-7}\right) \\ &= 4.27 \cdot 10^{-3}\ \text{J}. \end{aligned} \tag{4.9}$$

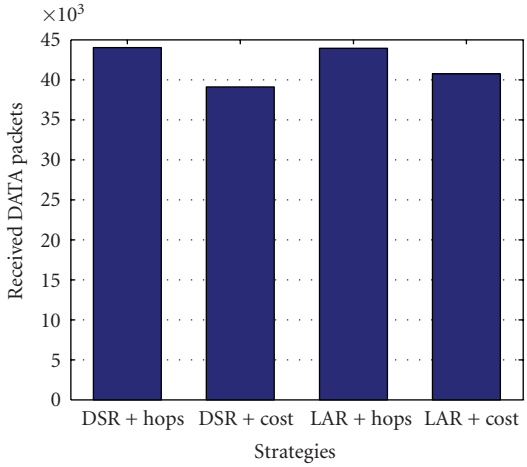

FIGURE 4.16. Received DATA packets for test case 1 with $R_{\text{TX-low}}$.

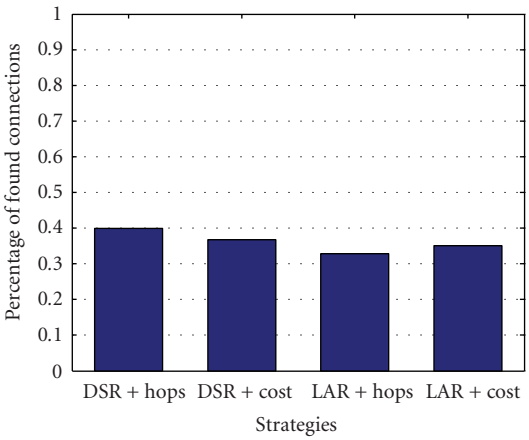

FIGURE 4.17. Percentage of found connections for test case 1 with $R_{\text{TX-low}}$.

If two hops over $d = 5$ m are used in place of the single hop, we get the overall cost:

$$\begin{aligned} E &= 4 \cdot E_{\text{start}} + 2 \cdot L \cdot \left(E_{\text{Rx-bit-fixed}} + E_{\text{Rx-bit-rate}}(R_b) + E_{\text{Tx-bit-rate}}(R_b)\right) \\ &\quad + 2 \cdot L \cdot \left(E_{\text{Tx-bit-prop}}(R_b) \cdot d^{\alpha}\right) \\ &= 1.104 \cdot 10^{-4} + 2 \cdot 5000 \cdot \left(7.17 \cdot 10^{-7}\right) + 2 \cdot 5000 \cdot \left(7.8125 \cdot 10^{-9}\right) \\ &= 7.35 \cdot 10^{-3}\ \text{J}, \end{aligned} \tag{4.10}$$

which is higher than the cost of the single hop at longer distance.

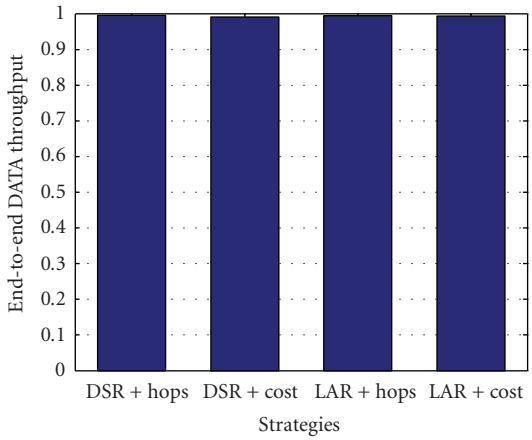

FIGURE 4.18. End-to-end DATA throughput for test case 1 with $R_{\text{TX-low}}$.

As far as routing algorithms are concerned, results show that, independently of the selected routing metric, the performance increase guaranteed by the adoption of LAR is far from dramatic. This can be explained by observing that the main advantage of LAR is the reduction of overhead by avoiding broadcast packets being forwarded in wrong directions. Under the condition of low connectivity, the number of broadcast packets is inherently limited by the low number of links available in the network, thus achieving the same effect pursued by LAR, at the price of a low percentage of found connections.

If we consider a higher transmission range, on the other hand, the above considerations are no longer valid, and we would thus expect an advantage in terms of network lifetime by adopting the power-aware cost function and the LAR protocol.

The results for transmission range set to $R_{\text{TX-med}}$ are presented in Figures 4.19 and 4.20 for found connections and delivered number of DATA packets, respectively. Results show that in both cases the LAR + cost strategy leads to the best performance, increasing by a factor of 2 both the number of found connections and the number of DATA packets. Furthermore, the adoption of the power-aware cost function leads to better performance independently of the selected routing algorithm.

Noticeably, also the short-term performance indicators, presented in Figures 4.21 and 4.22, are improved by the adoption of LAR routing and power-aware cost function.

The advantage of the LAR + cost solution is confirmed when the $R_{\text{TX-high}}$ transmission range is considered: Figure 4.23 shows that the number of found connections is increased by a factor of 2 by adopting the LAR + cost strategy.

The increase in found connections obtained by adopting the cost function is around 10%, as it was in the case of transmission range set to $R_{\text{TX-med}}$. This is coherent with the fact that, given the number of terminals and the size adopted in the

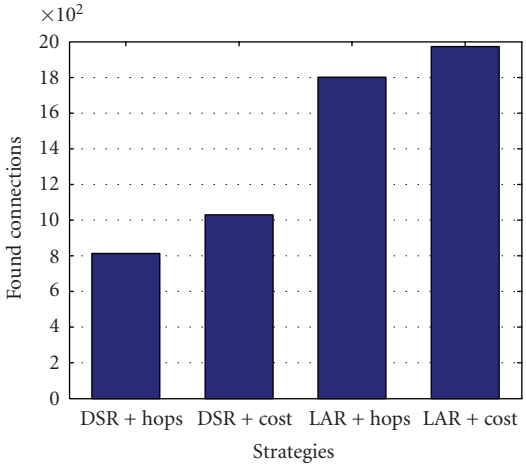

FIGURE 4.19. Found connections for test case 1 with $R_{\text{TX-med}}$.

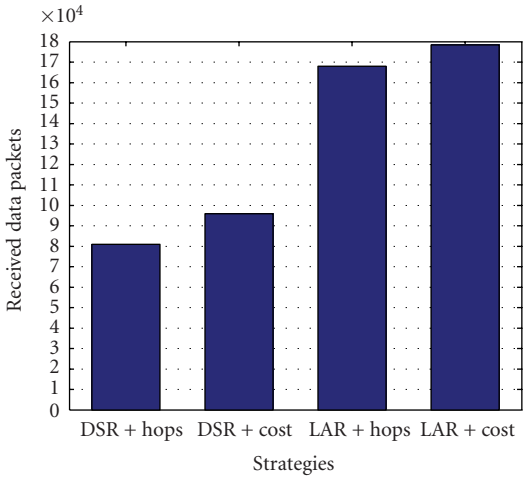

FIGURE 4.20. Received DATA packets for test case 1 with $R_{\text{TX-med}}$.

test cases, the average distance between two terminals is 40 m. As a consequence, the maximum advantage from the cost function is obtained when the transmission range reaches 40 m, that is, for $R_{\text{TX-med}}$. Further increases of the transmission range do not lead to any additional gain, since the energy saving obtained with the cost function is not related to the maximum transmission distance reachable by a terminal, but to the actual distance between terminals.

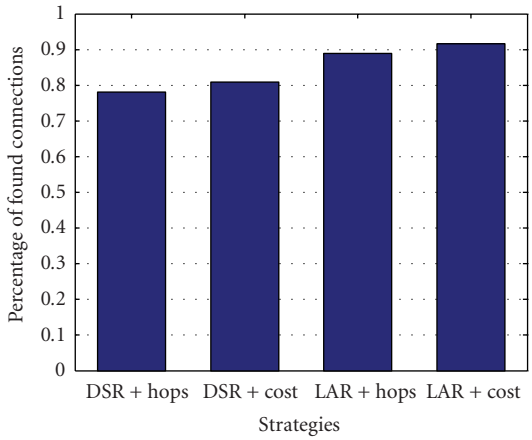

FIGURE 4.21. Percentage of found connections for test case 1 with $R_{\text{TX-med}}$.

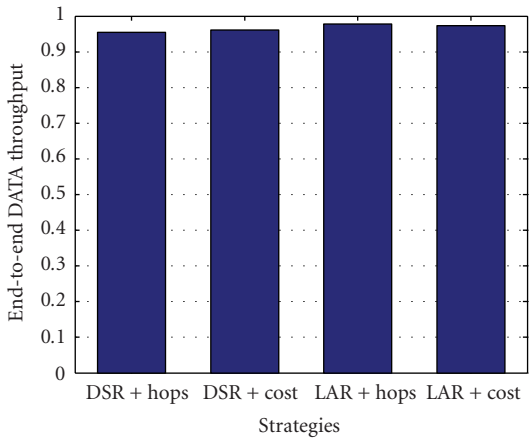

FIGURE 4.22. End-to-end DATA throughput for test case 1 with $R_{\text{TX-med}}$.

TABLE 4.3. Inertia mobility settings for test case 2.

Parameter	Value
V_{MAX}	6 m/s
ρ	0.5

4.5.3.2. Test case 2

This test case analyzed a scenario in which terminals were randomly deployed, and then moved following the *Inertia* mobility model, with mobility settings presented in Table 4.3.

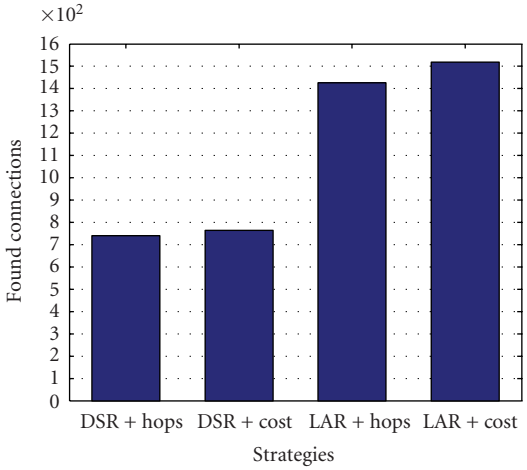

FIGURE 4.23. Found connections for test case 1 with $R_{\text{TX-high}}$.

The movement capability of terminals had a strong impact on network behavior, in particular in scenarios where network connectivity was more affected by mobility. This is the case when low transmission range $R_{\text{TX-low}}$ is considered: the introduction of mobility led indeed to results which are completely different from those obtained in test case 1 with still terminals.

Figure 4.24 shows the number of found connections in this scenario. It is evident that in this case, the introduction of the LAR algorithm increases network performance also with transmission range set to $R_{\text{TX-low}}$: in particular, the comparison between DSR + hops and LAR + hops shows an increase of about 20% in the number of found connections.

Note that in conditions of low connectivity and mobility, the adoption of cost instead of hops does not bring any advantage. As already observed for test case 1, in fact, the low transmission range leads in most cases to a higher energy consumption when moving from a single hop to two or more hops. In presence of mobility, furthermore, the cost-based strategies suffer from an additional increase of energy spent in signaling connection failures due to mobility by means of broadcast RRC packets. In fact, since the cost function leads to a higher average number of hops, as shown in Figure 4.25, the paths selected with this metric are more subject to failures caused by terminal mobility.

If we consider a transmission range set to $R_{\text{TX-med}}$, we observe, on the contrary, that the adoption of the cost function significantly increases the number of found connections. In this condition the best solution is thus the LAR + cost strategy, as shown in Figure 4.26.

This conclusion is also confirmed by the other long-term parameter, that is, the number of received DATA packets, shown in Figure 4.27.

The short-term parameters confirm that LAR + cost is overall the best choice: the throughput, presented in Figure 4.28, is almost identical for both LAR-based

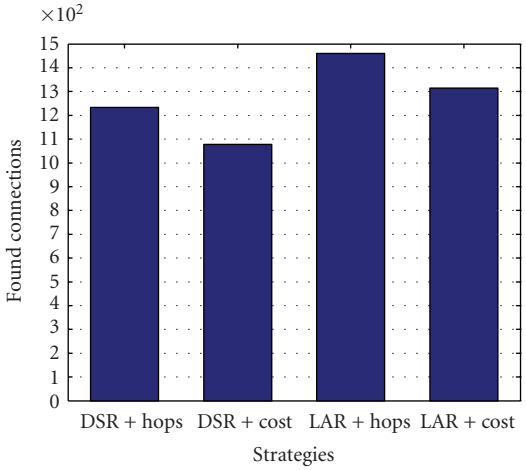

FIGURE 4.24. Found connections for test case 2 with $R_{\text{TX-low}}$.

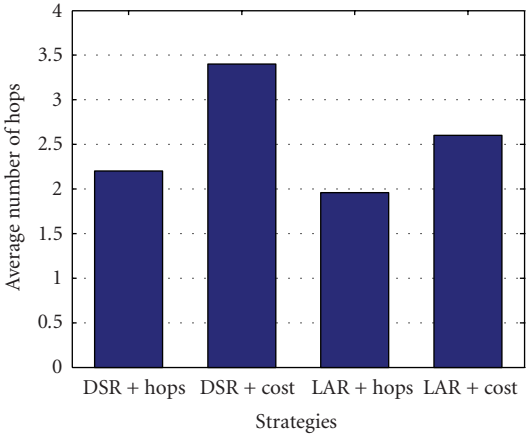

FIGURE 4.25. Average number of hops for test case 2 with $R_{\text{TX-low}}$.

strategies, and the same is true for the percentage of found connections, in Figure 4.29.

The advantage obtained by the LAR-based strategies on the short-term parameters is also influenced by the longer network lifetime. As an example, Figure 4.30 shows the evolution of the percentage of found connections over time for a single simulation run. The plot shows that the difference in the average value (Figure 4.29) is due to the capability of LAR-based strategies to keep the network in steady state for a longer period of time.

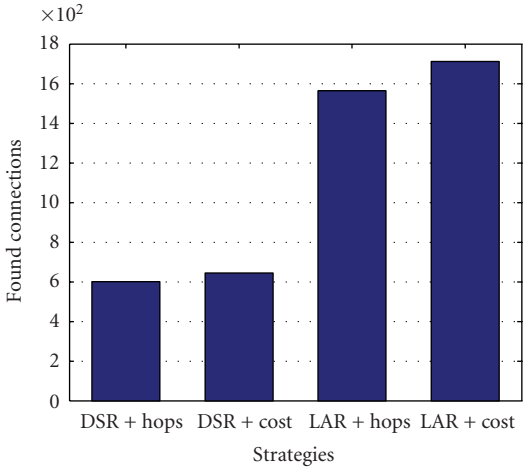

FIGURE 4.26. Found connections for test case 2 with $R_{\text{TX-med}}$.

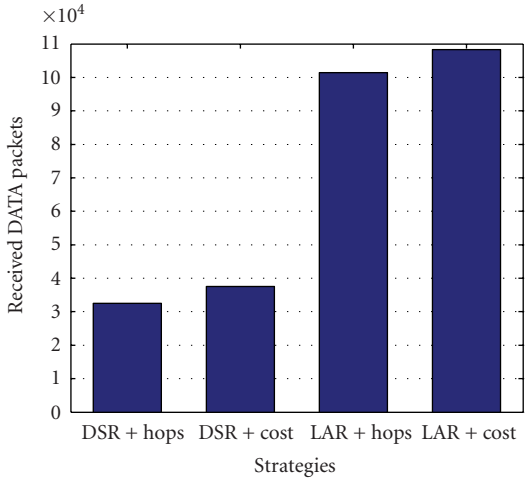

FIGURE 4.27. Received DATA packets for test case 2 with $R_{\text{TX-med}}$.

The case of high network connectivity confirms LAR-based strategies as the most efficient ones (see Figure 4.31), but in this case the performance gain achieved with the cost function is not significant.

This can be explained by considering that, as already observed for test case 1, an increase of transmission range over the average distance between two terminals does not bring any additional advantage for cost-based strategies. At the same time, the negative effect of connection failures due to mobility increases with transmission range, since RRC packets are transmitted at maximum power; this means that each RRC packet will consume higher energy, and that each packet will

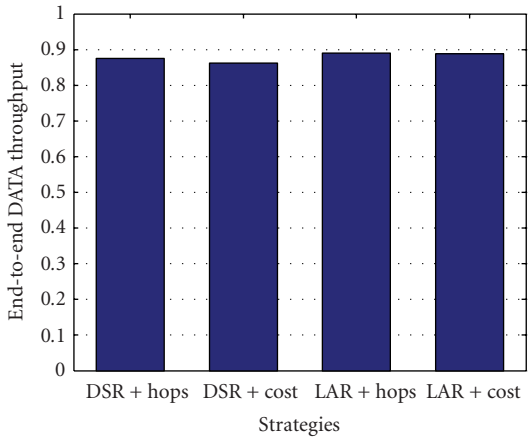

FIGURE 4.28. End-to-end DATA throughput for test case 2 with $R_{\text{TX-med}}$.

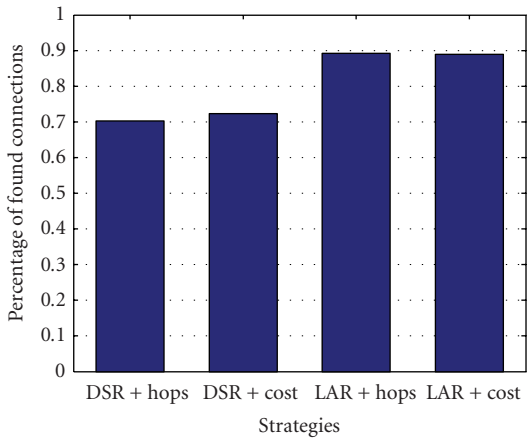

FIGURE 4.29. Percentage of found connections for test case 2 with $R_{\text{TX-med}}$.

be forwarded for a higher number of times, thanks to the higher network connectivity. As a consequence, the efficiency of cost-based strategies is reduced.

4.5.3.3. Test case 3

This test case analyzed a scenario in which terminals were randomly deployed, and then moved following the Kerberos mobility model, with mobility settings presented in Table 4.4.

The analysis of the performance of the four strategies in the case of the *Kerberos* mobility model is somewhat more difficult than in the other cases; the peculiar spatial distribution of terminals generated by this group mobility model must

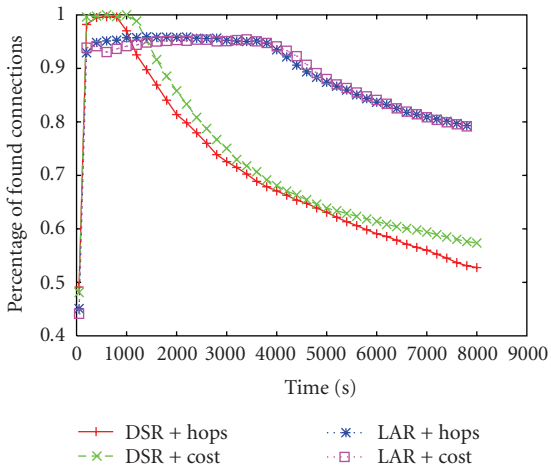

FIGURE 4.30. Percentage of found connections for test case 2 with $R_{\text{TX-med}}$ (single run).

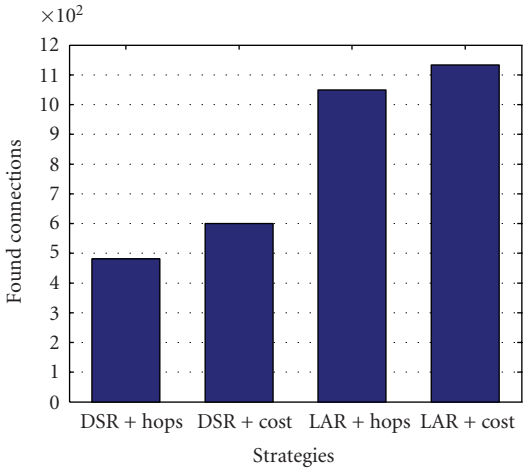

FIGURE 4.31. Found connections for test case 2 with $R_{\text{TX-high}}$.

be taken into account for a correct evaluation of the simulation results, and the distinction between intra and intergroup network topology properties must be considered.

The global number of found connections in the case of low transmission range is presented in Figure 4.32. The figure shows that, as much as in the case of test case 2, the presence of mobility allows for a higher network connectivity and thus leads to better results than in the case of still terminals. For all the four strategies, however, performance is significantly worse than in the case of the *Inertia* mobility model, as confirmed by the number of received DATA packets, presented in Figure 4.33.

Table 4.4. Kerberos mobility settings for test case 3.

Parameter	Value
V_{MAX}	6 m/s
Kerberos range	$R_{TX} - V_{MAX}/3$ m
N_{neigh}	4

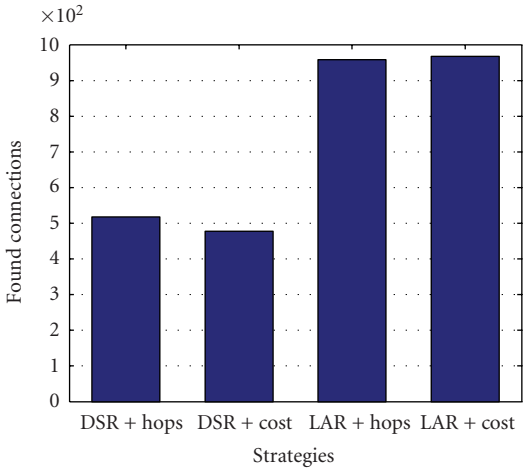

Figure 4.32. Found connections for test case 3 with $R_{TX\text{-}low}$.

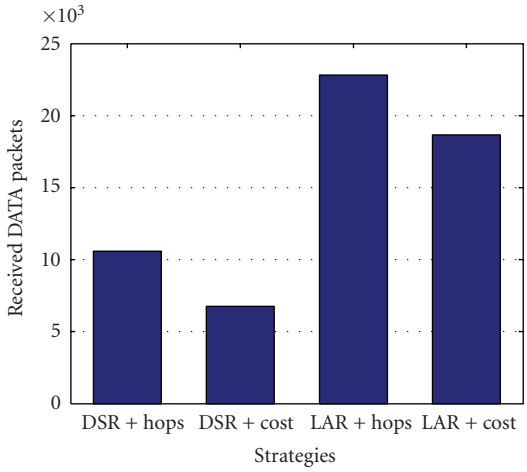

Figure 4.33. Received DATA packets for test case 3 with $R_{TX\text{-}low}$.

This is due to the fact that the *Kerberos* model does not lead to a uniform distribution of nodes, but creates groups of nodes. Figure 4.34 shows in fact the

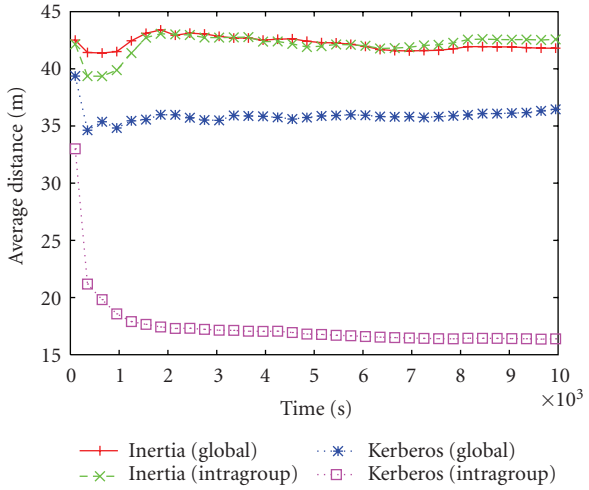

FIGURE 4.34. Average distances between two nodes in the network (global) and between two nodes in the same group (intragroup) for Inertia and Kerberos, the latter with Kerberos range = $R_{\text{TX-low}} - V_{\text{MAX}}/3$ m.

average distance between two nodes in the network and the average distance between two nodes in the same group for both *Inertia* and *Kerberos*. As one could expect, the two distances are similar in the case of *Inertia*, since no special group behavior is defined in the model. Oppositely, in the case of *Kerberos* a large difference between the two values can be observed.

The lower performance observed for all strategies in test case 3 is due to the higher connectivity which characterizes the *Kerberos* model. Results in Section 4.5.2.5 show in fact that this mobility model guarantees a higher average connectivity than the *Inertia* model; this translates in a higher number of forwarded RRQ packets, and thus a shorter network lifetime. The higher connectivity, on the other hand, leads to a better performance the short term, as presented in Figure 4.35, showing the percentage of found connections for the first 5000 seconds of a simulation run for the same strategy (DSR + hops) with the two mobility models.

The higher network connectivity also determines in this test case a larger performance gap between DSR and LAR-based strategies. The average increase in number of found connections obtained by switching to LAR is in fact in the order of 100% for test case 3, whereas it was only around 20% in test case 2 with the same settings (see Figure 4.24).

Note that the cost-based strategies are penalized by both the short transmission range and the negative effect of mobility on route duration, and achieve thus lower performance than the hop-based strategies, similarly to what was observed in test cases 1 and 2.

The results with medium transmission range $R_{\text{TX-med}}$, presented in Figures 4.36 and 4.37, confirm that the adoption of the LAR strategies increases the network lifetime. In this case too, the adoption of the cost-based metric has a negative

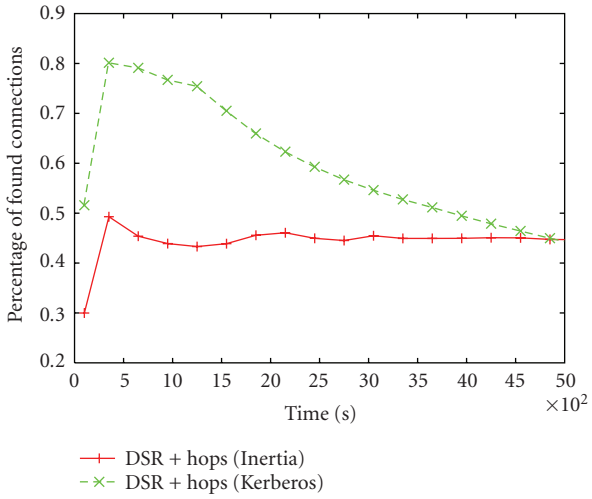

FIGURE 4.35. Percentage of found connections in a single simulation run for the DSR + hops strategy with Inertia and Kerberos mobility models.

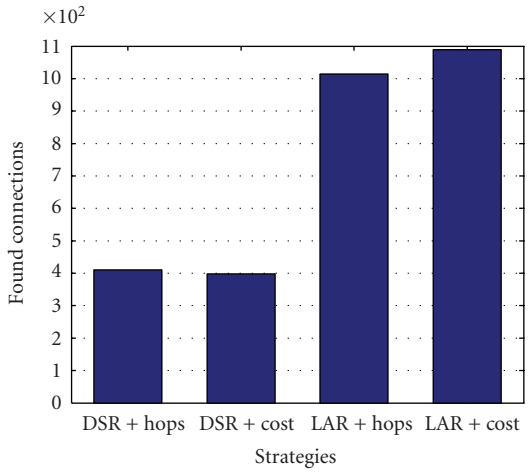

FIGURE 4.36. Found connections for test case 3 with $R_{\text{TX-med}}$.

effect on network performance, so that the LAR + hops strategy is still the overall best solution in this scenario. Note that this conclusion differs from what was obtained for the same transmission range in test cases 1 and 2. In particular, in test case 2 the negative effect of mobility was compensated by the energy saving achieved with a higher number of hops, so that for the transmission range $R_{\text{TX-med}}$, the LAR + cost led to the best performance (Figure 4.26). This is no longer true in test case 3, due the peculiar mobility pattern characterizing the *Kerberos* model. In

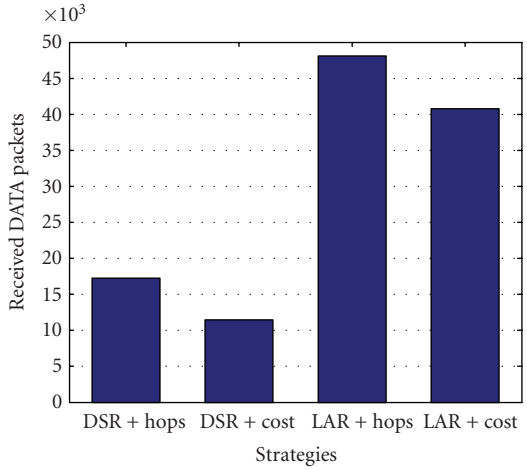

FIGURE 4.37. Received DATA packets for test case 3 with $R_{\text{TX-med}}$.

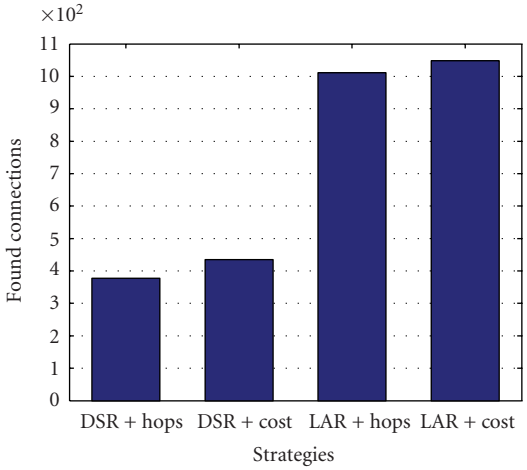

FIGURE 4.38. Found connections for test case 3 with $R_{\text{TX-high}}$.

Section 4.5.2.5 it was show in fact that the *Kerberos* mobility model is characterized by a shorter intergroup link duration if compared to *Inertia*: as a consequence, the adoption of intergroup links in a connection has a stronger negative effect on route stability. The cost-based strategies are more sensible to this effect, since the selected routes are characterized by a high number of hops, and there is thus a significant probability for a route to include one or more intergroup links. The lower route stability is clearly indicated by the fact that, despite the highest number of found connections, the LAR + cost strategy is capable of delivering a lower number of DATA packets than the LAR + Hops strategy: this is due to the fact that

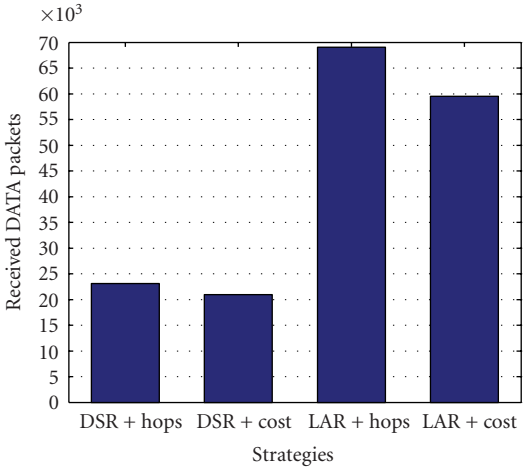

FIGURE 4.39. Received DATA packets for test case 3 with $R_{\text{TX-high}}$.

routes selected with the LAR + cost strategy have a shorter duration and thus the corresponding connections are able to deliver a lower number of packets before being broken for a lack of connectivity.

Results with high transmission range $R_{\text{TX-high}}$ (Figures 4.38 and 4.39) further confirm that cost-based strategies are heavily affected by the mobility pattern of the *Kerberos* model. Although in fact the higher network connectivity allows a higher average number of packets to be delivered in each connection for all the four strategies, yet a significant gap can be observed between hop-based and cost-based strategies.

Quite interestingly, as the transmission range (and consequently the *Kerberos Range*) increases, the results in test case 3 approach those obtained in test case 2; this is coherent with the fact that, as the Kerberos range increases, there is a lower and lower probability for a node to remain isolated from its own group and thus to be forced to modify its mobility pattern. As a consequence, the *Kerberos* mobility model will fall back more and more to the standard *Inertia* mobility model.

4.5.4. Conclusions

The analysis carried out throughout this section had the objective of testing the effectiveness of the location-based, power-aware approach for MAC and routing in low bit rate UWB networks introduced in the previous sections of this chapter.

The results of such analysis highlight that the exploitation of ranging and locationing information provided by the UWB physical layer may effectively extend network lifetime without significant effects on short-term network performance.

The analysis also pointed out the direct relation between the scenario in which the network is deployed and the performance of the selected routing strategy. In particular, network connectivity, transmission range, and mobility pattern of the

nodes are all factors which can influence the performance of a routing strategy and, most important, may have a different effect on different strategies.

Results showed in fact that, depending on the scenario, the best network performance can be obtained by means of either a full exploitation of the positional information provided by UWB in both routing algorithm and metric (as in test cases 1 and 2), or a partial one, limited to the adoption of the location information in the routing algorithm (as in test case 3).

The flexibility guaranteed by the cost function defined in Section 4.1, however, enables a smooth transition from a fully power-aware metric to a traditional hop-based metric, and thus allows for a fine adaptation of the MAC and routing strategy to any network scenario, ranging between the two extreme cases of sparse networks of fixed nodes and dense networks of highly mobile nodes.

Bibliography

[1] M.-G. Di Benedetto and G. Giancola, *Understanding Ultra Wide Band Radio Fundamentals*, Prentice Hall, Upper Saddle River, NJ, USA, 2004.

[2] M.-G. Di Benedetto and B. Vojcic, "Ultra wide band wireless communications : a tutorial," *Journal of Communications and Networks*, vol. 5, no. 4, pp. 290–302, 2003.

[3] M. Z. Win and R. A. Scholtz, "Ultra-wide bandwidth time-hopping spread-spectrum impulse radio for wireless multiple-access communications," *IEEE Transactions on Communications*, vol. 48, no. 4, pp. 679–689, 2000.

[4] L. De Nardis and M.-G. Di Benedetto, "Medium access control design for UWB communication systems: review and trends," *Journal of Communications and Networks*, vol. 5, no. 4, pp. 386–393, 2003.

[5] Federal Communications Commission, "Revision of Part 15 of the Commission's rules regarding ultra-wideband transmission systems," Report 98–153, Federal Communications Commission, Washington D.C., USA, 2002.

[6] P. Karn, "MACA—A new channel access protocol for packet radio," in *Proceedings of ARRL/CRRL Amateur Radio Ninth Computer Networking Conference*, pp. 134–140, Ontario, Canada, September 1990.

[7] V. Bharghavan, A. Demers, S. Shenker, and L. Zhang, "MACAW: A media access protocol for wireless LANs," in *Proceedings of Conference on Applications, Technologies, Architectures and Protocols for Computer Communication (SIGCOMM '94)*, pp. 212–225, London, UK, August–September 1994.

[8] F. Talucci and M. Gerla, "MACA-BI (MACA by invitation). A wireless MAC protocol for high speed ad hoc networking," in *Proceedings of 6th IEEE International Conference on Universal Personal Communications Record*, vol. 2, pp. 913–917, San Diego, Calif, USA, 1997.

[9] C. L. Fullmer and J. J. Garcia-Luna-Aceves, "Floor acquisition multiple access (FAMA) for packet radio networks," in *Proceedings of Conference on Applications, Technologies, Architectures and Protocols for Computer Communication (SIGCOMM '95)*, pp. 262–273, Cambridge, Mass, USA, August–September 1995.

[10] B. P. Crow, I. Widjaja, J. G. Kim, and P. T. Sakai, "IEEE 802.11 wireless local area networks," *IEEE Communications Magazine*, vol. 35, no. 9, pp. 116–126, 1997.

[11] F. A. Tobagi and L. Kleinrock, "Packet switching in radio channels: part II—The hidden terminal problem in carrier sense multiple access and the busy tone solution," *IEEE Transactions on Communications*, vol. 23, no. 12, pp. 1417–1433, 1975.

[12] J. Deng and Z. J. Haas, "Dual busy tones multiple access (DBTMA): a new medium access control for packet radio networks," in *Proceedings of IEEE International Conference on Universal Personal Communications (ICUPC '98)*, vol. 2, pp. 973–977, Florence, Italy, October 1998.

[13] S. Singh and C. S. Raghavendra, "PAMAS: Power aware multiaccess protocol with signalling for ad hoc networks," *ACM Computer Communication Review*, vol. 28, no. 3, pp. 5–26, 1998.

[14] C.-K. Toh, "Maximum battery life routing to support ubiquitous mobile computing in wireless ad hoc networks," *IEEE Communications Magazine*, vol. 39, no. 6, pp. 138–147, 2001.

[15] M.-G. Di Benedetto and P. Baldi, "A model for self-organizing large-scale wireless networks," in *Proceedings of International Workshop on 3G Infrastructure and Services*, pp. 210–213, Athens, Greece, July 2001.

[16] L. De Nardis, P. Baldi, and M.-G. Di Benedetto, "UWB ad-hoc networks," in *Proceedings of IEEE Conference on Ultra Wideband Systems and Technologies (UWBST '02)*, pp. 219–223, Baltimore, Md, USA, May 2002.

[17] P. Baldi, L. De Nardis, and M.-G. Di Benedetto, "Modeling and optimization of UWB communication networks through a flexible cost function," *IEEE Journal on Selected Areas in Communications*, vol. 20, no. 9, pp. 1733–1744, 2002.

[18] B. Karp and H. T. Kung, "Gpsr: greedy perimeter stateless routing for wireless networks," in *Proceedings of 6th ACM/IEEE International Conference on Mobile Computing and Networking (ACM MOBICOM '00)*, pp. 243–254, Boston, Mass, USA, August 2000.

[19] D. Kim, Y. Choi, and C. K. Toh, "Location-aware long lived-route selection in wireless ad hoc network," in *IEEE 52nd Vehicular Technology Conference (VTC '00)*, vol. 4, pp. 1914–1919, Boston, Mass, USA, September 2000.

[20] S. Basagni, I. Chlamtac, V. R. Syrotiuk, and B. A. Woodward, "A distance routing effect algorithm for mobility (DREAM)," in *Proceedings of ACM/IEEE International Conference on Mobile Computing and Networking (ACM MOBICOM '98)*, pp. 76–84, Dallas, Tex, USA, 1998.

[21] Y.-B. Ko and N. H. Vaidya, "Location-aided routing (LAR) in mobile ad hoc networks," in *Proceedings of 4th Annual ACM/IEEE International Conference on Mobile Computing and Networking (MOBICOM '98)*, pp. 66–75, Dallas, Tex, USA, October 1998.

[22] Y.-B. Ko and N. H. Vaidya, "Optimizations for location-aided routing (LAR) in mobile ad hoc networks," Tech. Rep. 98-023, CS Department, Texas A & M University, Dallas, Tex, USA, 1998.

[23] S. Capkun, M. Hamdi, and J. P. Hubaux, "GPS-free positioning in mobile Ad-Hoc networks," in *Proceedings of 34th Annual Hawaii International Conference On System Sciences*, pp. 3481–3490, Maui, Hawaii, USA, January 2001.

[24] D. B. Johnson and D. A. Maltz, "Dynamic source routing in ad hoc wireless networks," in *Mobile Computing*, vol. 353, pp. 153–181, Kluwer Academic Publishers, Dordrecht, The Netherlands, 1996.

[25] D. P. Bertsekas and R. Gallager, *Data Networks*, Prentice Hall, Englewood Cliffs, NJ, USA, 2nd edition, 1992.

[26] M.-G. Di Benedetto, L. De Nardis, M. Junk, and G. Giancola, "$(\text{UWB})^2$: uncoordinated, wireless, baseborn medium access for UWB communication networks," *Springer Mobile Networks and Applications*, vol. 10, no. 5, pp. 663–674, 2005.

[27] D. Raychaudhuri, "Performance analysis of random access packet-switched code division multiple access systems," *IEEE Transactions on Communications*, vol. 29, no. 6, pp. 895–901, 1981.

[28] S. Dastangoo, B. R. Vojcic, and J. N. Daigle, "Performance analysis of multi-code spread slotted ALOHA (MCSSA) system," in *Proceedings of IEEE Global Telecommunications Conference (GLOBECOM '98)*, vol. 3, pp. 1839–1847, Sydney, NSW, Australia, November 1998.

[29] E. S. Sousa and J. A. Silvester, "Spreading code protocols for distributed spread-spectrum packet radio networks," *IEEE Transactions on Communications*, vol. 36, no. 3, pp. 272–281, 1988.

[30] M. S. Iacobucci and M.-G. Di Benedetto, "Computer method for pseudo-random codes generation," National Italian patent, RM2001A000592.

[31] Y.-C. Hu and D. B. Johnson, "Caching strategies in on-demand routing protocols for wireless ad hoc networks," in *Proceedings of 6th Annual International Conference on Mobile Computing and Networking (MOBICOM '00)*, pp. 231–242, Boston, Mass, USA, August 2000.

[32] E. M. Royer, P. M. Melliar-Smith, and L. E. Moser, "An analysis of the optimum node density for ad hoc mobile networks," in *Proceedings of IEEE International Conference on Communications (ICC '01)*, vol. 3, pp. 857–861, Helsinki, Finland, June 2001.

[33] B. Liang and Z. J. Haas, "Predictive distance-based mobility management for multidimensional PCS networks," *IEEE/ACM Transactions on Networking*, vol. 11, no. 5, pp. 718–732, 2003.

[34] S. Basagni, I. Chlamtac, and V. R. Syrotiuk, "Dynamic source routing for ad hoc networks using the global positioning system," in *Proceedings of IEEE Wireless Communications and Networking Conference (WCNC '99)*, vol. 1, pp. 301–305, New Orleans, La, USA, September 1999.

[35] M. Bergamo, R. Hain, K. Kasera, D. Li, R. Ramanathan, and M. Steenstrup, "System design specification for mobile multimedia wireless network (MMWN) (draft)," Tech. Rep., DARPA project DAAB07-95C -D156, October 1996.

[36] X. Hong, M. Gerla, G. Pei, and C.-C. Chiang, "A group mobility model for ad hoc wireless networks," in *Proceedings of 2nd ACM International Workshop on Modeling and Simulation of Wireless and Mobile Systems (MSWiM '99)*, pp. 53–60, Seattle, Wash, USA, August 1999.

[37] K. H. Wang and B. Li, "Group mobility and partition prediction in wireless ad-hoc networks," in *Proceedings of IEEE International Conference on Communications (ICC '02)*, vol. 2, pp. 1017–1021, New York, NY, USA, April–May 2002.

[38] F. Bai, N. Sadagopan, and A. Helmy, "Important: a framework to systematically analyze the impact of mobility on performance of routing protocols for adhoc networks," in *Proceedings of 22nd Annual Joint Conference of the IEEE Computer and Communications Societies (INFOCOM '03)*, vol. 2, pp. 825–835, San Francisco, Calif, USA, March–April 2003.

[39] R. Min and A. Chandrakasan, "A framework for energy-scalable communication in high-density wireless networks," in *Proceedings of International Symposium on Low Power Electronics and Design (ISLPED '02)*, pp. 36–41, Monterey, Calif, USA, August 2002.

Maria-Gabriella Di Benedetto: INFOCOM Department, School of Engineering, University of Rome La Sapienza, 00184 Rome, Italy

Email: gaby@infocom.ing.uniroma1.it

Luca De Nardis: INFOCOM Department, School of Engineering, University of Rome La Sapienza, 00184 Rome, Italy

Email: lucadn@newyork.ing.uniroma.it

Salvatore Falco: INFOCOM Department, School of Engineering, University of Rome La Sapienza, 00184 Rome, Italy

Email: sfalco@newyork.ing.uniroma1.it